Improved XTZ masses and mass ratios from Laplace sum rules at NLO

R. Albuquerque, S. Narison, D. Rabetiarivony

Available online at www.sciencedirect.com

ScienceDirect

Nuclear Physics A 1023 (2022) 122451

NUCLEAR PHYSICS A

www.elsevier.com/locate/nuclphysa

Improved XTZ masses and mass ratios from Laplace sum rules at NLO

R. Albuquerque [a], S. Narison [b,c,*], D. Rabetiarivony [c]

[a] *Faculty of Technology, Rio de Janeiro State University (FAT, UERJ), Brazil*
[b] *Laboratoire Univers et Particules de Montpellier (LUPM), CNRS-IN2P3, Case 070, Place Eugène Bataillon, 34095 Montpellier, France*
[c] *Institute of High-Energy Physics of Madagascar (iHEPMAD), University of Ankatso, Antananarivo 101, Madagascar*

Received 31 January 2022; received in revised form 30 March 2022; accepted 7 April 2022
Available online 15 April 2022

Abstract

We present improved estimates of the couplings, masses and mass ratios of the Z_Q, X_Q and $T_{QQ\bar{q}\bar{q}'}$ states ($Q \equiv c, b$; $q, q' \equiv u, d, s$) using (inverse) QCD Laplace sum rules (LSR), their ratios $\mathcal{R}$ and double ratios DRSR within stability criteria, where the NLO factorized PT QCD corrections are included which is important for giving a meaning on the running $\overline{MS}$ heavy quark mass used in the analysis. We show that combined $\mathcal{R}$ and DRSR can provide more precise results. In the 1st part of the paper, we conclude that the observed $X_c(3872)$ and $Z_c(3900)$ are *tetramoles* states (superposition of quasi-degenerated molecule and a tetraquark states having (almost) the same coupling to the currents) with the predicted masses: $M_{\mathcal{T}_{X_c}} = 3876(44)$ MeV and $M_{\mathcal{T}_{Z_c}} = 3900(42)$ MeV. In the 2nd part, we focus on the analysis of the four-quark nature of different $T_{QQ\bar{q}\bar{q}'}$ 1^+ and 0^+ states within the $\bar{3}_c 3_c$ interpolating currents. The final results from $\mathcal{R}$ and $\mathcal{R} \oplus$ DRSR are summarized in Table 7. Combined $\mathcal{R}$ and DRSR calibrated to the observed $X_c(3872)$ lead to a precise prediction of e.g. $M_{T_{cc}^{1^+}} = 3886(6)$ MeV. In a similar way, the DRSR for the $M_{T_{cc}^{0^+}}/M_{T_{cc}^{1^+}}$ calibrated to $M_{T_{cc}^{1^+}}$ gives $M_{T_{cc}^{0^+}} = 3883(3)$ MeV. The SU3 breaking ratios $M_{T_{cc\bar{s}\bar{s}}^{0^+}}/M_{T_{cc}^{0^+}}$ lead to the improved mass predictions: $M_{T_{cc\bar{s}\bar{s}}^{0^+}} = 3988(12)$ MeV. In the 3rd part, the analysis is extended to the beauty mesons, where we find the tetramole masses: $M_{\mathcal{T}_{Z_b}} = 10579(99)$ MeV and $M_{X_b} = 10545(131)$ MeV. We also observe that the $T_{bb\bar{q}\bar{q}'}^{1^+,0^+}$ $(q, q' \equiv u, d, s)$ states are (almost) stable

* Corresponding author at: Laboratoire Univers et Particules de Montpellier (LUPM), CNRS-IN2P3, Case 070, Place Eugène Bataillon, 34095 Montpellier, France.
E-mail addresses: raphael.albuquerque@uerj.br (R. Albuquerque), snarison@yahoo.fr (S. Narison), rd.bidds@gmail.com (D. Rabetiarivony).

https://doi.org/10.1016/j.nuclphysa.2022.122451

(within the errors) against strong interactions. In the 4th part, we (critically) review and correct some recent LSR estimates of the $T^{1^+,0^+}_{QQ\bar{q}\bar{q}'}$ masses. Our combined LSR $\oplus$ DRSR results are confronted with the ones from some other approaches (lattices and quark models) in Fig. 26.

Keywords: QCD spectral sum rules; Perturbative and non-perturbative QCD; Exotic hadrons; Masses and decay constants

1. Introduction

Beyond the successful quark model of Gell-Mann [1] and Zweig [2], Rossi and Veneziano have introduced the four-quark states within the string model [3] in order to describe baryon-antibaryon scattering, while Jaffe [4] has introduced them within the bag models for an attempt to explain the complex structure of the $I = 1, 0$ light scalar mesons (see also [5–11]).[1]

In a series of papers [17–24], we have used QCD spectral sum rules (QSSR) à la SVZ [25,26][2] within stability criteria to estimate the masses and couplings of different exotic XYZ states. Compared to the existing papers in the literature, we have emphasized that the inclusion of PT radiative corrections is important for justifying the choice of the input value of the heavy quark mass which plays a capital role in the analysis. In so doing, we have observed that, in the $\overline{MS}$ scheme, this correction is tiny which *a posteriori* explains the success of these LO results using the quark mass value in this scheme.

More recently, we have applied the LSR [25,38,39] for interpreting the new states around (6.2–6.9) GeV found by the LHCb-group [40] to be a doubly/fully hidden-charm molecules $(\bar{Q}Q)(Q\bar{Q})$ and $(\bar{Q}\bar{Q})(QQ)$ tetraquarks states [21], while the new states found by the same group from the DK invariant mass [41] have been interpreted by a 0^+ and 1^- tetramoles (superposition of almost degenerate molecules and tetraquark states having the same quantum numbers and almost the same couplings) slightly mixed with their radial excitations [22]. We have also systematically studied the Z_c-like spectra and interpreted the $Z_c(3900)$ and the $Z_{cs}(3983)$ state found by BESIII [42] as good candidates for (1^+) tetramole states [23].

Motivated by the recent LHCb discovery of a 1^+ state at 3875 MeV [43], just below the D^*D threshold, which is a good isoscalar ($I = 0$) $T_{cc\bar{u}\bar{d}}$ axial vector ($J^P = 1^+$) candidate, we improve in this paper the existing QSSR results by combining the direct mass determinations from the ratios $\mathcal{R}$ of Inverse Laplace sum rule (LSR) with the ratio of masses from the double ratio of sum rules (DRSR). In so doing, we start by improving the previous estimate of mass and coupling of the $X_c(3872)$ which will serve as an input in our DRSR approach. We complete our analysis by studying the SU3 breakings for $T_{cc\bar{s}\bar{s}}$ and $T_{cc\bar{s}\bar{u}}$ states. Finally, we extend the whole study to the case of the $T_{bb\bar{q}\bar{q}'}$ states. Our results are confronted with the existing LSR results and the ones from some other approaches which are briefly reviewed.

[1] See however [12–16] for a gluonium interpretation of the light $I = 0$ scalar mesons.
[2] For reviews, see e.g. [27–37].

2. The QCD inverse Laplace sum rules (LSR) approach

We shall be concerned with the two-point correlator:

$$\Pi^{\mu\nu}_{\mathcal{H}}(q^2) = i\int d^4x\, e^{iqx}\langle 0|\mathcal{T}\mathcal{O}^{\mu}_{\mathcal{H}}(x)\left(\mathcal{O}^{\nu}_{\mathcal{H}}(0)\right)^{\dagger}|0\rangle$$
$$\equiv -\left(g^{\mu\nu}-\frac{q^{\mu}q^{\nu}}{q^2}\right)\Pi^{(1)}_{\mathcal{H}}(q^2)+\frac{q^{\mu}q^{\nu}}{q^2}\Pi^{(0)}_{\mathcal{H}}(q^2) \tag{1}$$

built from the local hadronic operators $\mathcal{O}^{\mu}_{\mathcal{H}}(x)$ (see Table 1). It obeys the Finite Energy Inverse Laplace Transform Sum Rule (LSR) and their ratios:

$$\mathcal{L}^c_n|_{\mathcal{H}}(\tau,\mu) = \int_{(2M_c+m_q+m_{q'})^2}^{t_c} dt\, t^n\, e^{-t\tau}\frac{1}{\pi}\text{Im}\,\Pi^{(1,0)}_{\mathcal{H}}(t,\mu)\,:\,n=0,1\,; \qquad \mathcal{R}^c_{\mathcal{H}}(\tau)=\frac{\mathcal{L}^c_1|_{\mathcal{H}}}{\mathcal{L}^c_0|_{\mathcal{H}}}, \tag{2}$$

where $q, q' \equiv u, d, s$, M_c is the on-shell/pole charm quark mass and $m_{q,q'}$ (we shall neglect u, d quark masses) the running strange quark mass, τ is the LSR variable, t_c is the threshold of the "QCD continuum" which parametrizes, from the discontinuity of the Feynman diagrams, the spectral function $\text{Im}\,\Pi_{\mathcal{H}}(t, m_c^2, m_s^2, \mu^2)$. In the minimal duality ansatz which we shall use in this paper[3]:

$$\frac{1}{\pi}\text{Im}\,\Pi^{(1,0)}_{\mathcal{H}}(t) = f^2_{\mathcal{H}}M^8_{\mathcal{H}}\,\delta(t-M^2_{\mathcal{H}})+\frac{1}{\pi}\text{Im}\,\Pi^{(1,0)}_{\mathcal{H}}(t)|_{\text{QCD}}\,\theta(t-t_c), \tag{3}$$

one can deduce the mass squared from the ratio of LSR at the optimization point τ_0:

$$\mathcal{R}^c_{\mathcal{H}}(\tau_0) = M^2_{\mathcal{H}}. \tag{4}$$

We shall also work with the double ratio of sum rule (DRSR) [45]:

$$r_{\mathcal{H}'/\mathcal{H}}(\tau_0) \equiv \sqrt{\frac{\mathcal{R}^c_{\mathcal{H}'}}{\mathcal{R}^c_{\mathcal{H}}}} = \frac{M_{\mathcal{H}'}}{M_{\mathcal{H}}}, \tag{5}$$

which can be free from systematics provided that $\mathcal{R}^c_{\mathcal{H}}$ and $\mathcal{R}^c_{\mathcal{H}'}$ optimize at the same values of τ and of t_c:

$$\tau_0|_{\mathcal{H}} \simeq \tau_0|_{\mathcal{H}'}\,, \qquad t_c|_{\mathcal{H}} \simeq t_c|_{\mathcal{H}'}\,. \tag{6}$$

This DRSR has been used in different channels for predicting successfully the few MeV mass-splittings (SU3-breakings, parity splittings,...) between different hadrons [45–51]. In particular, it has been used for four-quark and molecule states in [49–51]. In this paper, we extend the previous analysis for improving the existing mass predictions of the X_Q, Z_Q and $T_{QQ\bar{q}\bar{q}}$ states and for giving a correlation among them. We also predict the mass-splittings due to SU3 breakings and to spin and parity for the $T_{QQ\bar{q}\bar{q}'}$ states.

[3] Parametrization beyond the minimal duality ansatz ⊕ uses of high degree moments have been considered in [22–24] to estimate the masses of the 1st radial excitation of four-quark/molecule states and in [12,44] for studying the gluonia spectra.

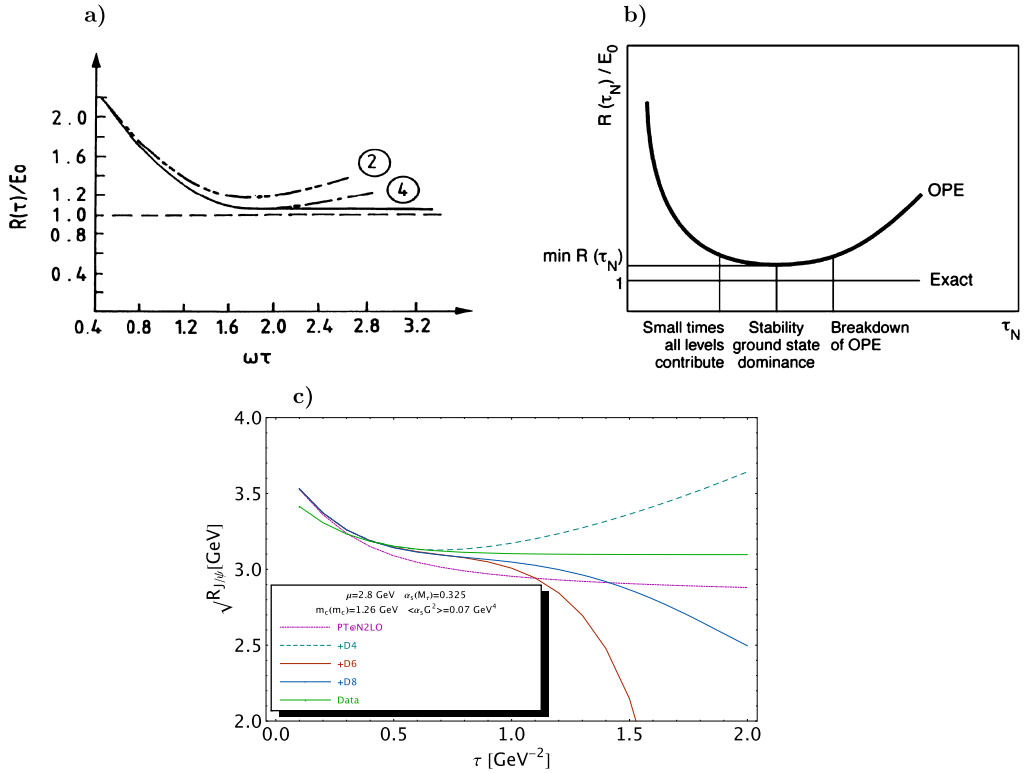

Fig. 1. a) Harmonic oscillator state for each given truncation of the series compared to the exact solution (horizontal line); b) Schematic presentation of stability of the charmonium ratio of moments; c) Explicit analysis of the J/ψ systems moment for different truncation of the OPE from e.g. [52].

3. The stability criteria for extracting the optimal results

In the LSR analysis, we have three external variables: the LSR variable $\tau \equiv 1/M_B^2$ where M_B is the original variable used by SVZ [25], the QCD continuum threshold t_c and the subtraction point μ. One considers that physical observables like the masses and meson couplings should be independent/minimal sensitive on these parameters.

- The τ-stability

It has been studied from the example of the harmonic oscillator in quantum mechanics [33,38] and from its analogue charmonium non-relativistic form of the LSR shown in Fig. 1. A such quantum mechanic example has been explicitly checked for vector charmonium and bottomium systems where complete data are available (see e.g. [52] and the J/ψ systems in Fig. 1) and in many other examples in [27,28] and different original papers by the authors.

At this τ stability point where there is a balance between the low and high-energy region, one can check the lowest ground state dominance of the LSR and the convergence of the OPE.

- The t_c-stability

The QCD continuum threshold t_c is (in principle) a free parameter in the analysis though one (intuitively) expects it to be around the mass of the first excitation which cannot be accurate as the

QCD continuum is supposed to smear all higher radial excitations contributions to the spectral function.

To be conservative we take t_c from the beginning of τ-stability until the beginning of t_c-stability [27–29] where the t_c-stability region corresponds to a complete dominance of the lowest ground state in the QSSR analysis. This conservative range of t_c-values is larger than the usual choice done in the current literature which is often done at the lowest values of t_c where one starts to have the τ-stability.

- The μ-stability

This is used to fix in a rigorous optimal way, the arbitrary substraction constant appearing in the PT calculation of the Wilson coefficients and in the QCD input renormalized parameters. We have observed in our previous analysis for the four-quark and molecule states [18,22–24] that its value is (almost) universal:

$$\mu_c \simeq 4.65(5)\ \text{GeV}\ , \qquad \mu_b \simeq 5.20(5)\ \text{GeV}, \tag{7}$$

respectively for the charm and beauty states. We shall check this result explicitly in the next sections.

One can also alternatively eliminate the μ-dependence of the result, by working with the resummed quantity after applying the homogeneous Renormalization Group equation (RGE) obeyed by the QCD expression of the LSR which is superconvergent:

$$\Big\{ -\frac{\partial}{\partial t} + \beta(\alpha_s)\alpha_s \frac{\partial}{\partial \alpha_s} - \sum_i (1+\gamma_m(\alpha_s)x_i \frac{\partial}{\partial x_i} \Big\} \mathcal{L}_n^c(e^t\tau, \alpha_s, x_i, \mu) = 0\ , \tag{8}$$

where $t \equiv (1/2)L_\tau$, $x_i \equiv m_i/\mu$. The renormalization group improved (RGI) solution is:

$$\mathcal{L}_n^c(e^t\tau, \alpha_s, x_i) = \mathcal{L}_n^c(t=0, \bar{\alpha}_s(\tau), \bar{x}_i(\tau))\ , \tag{9}$$

where $\bar{\alpha}_s(\tau)$ and $\bar{x}_i(\tau)$ are the running QCD coupling and mass. However, the RGE solution $\mu^2 = 1/\tau$ corresponds to lower values of $\mu \approx 1.6$ GeV where the convergence of the PT series is slower than in the previous case in Eq. (7).

An explicit comparison of the results from these two ways can be found in [57]. However, one should remark that the choice $\mu^2 = 1/\tau$ corresponds to a value of μ lower than the optimized one in Eq. (7) where NLO corrections are larger.

- Importance of the Figures in the analysis

We emphasize the importance for showing the different figures for each channel though having similar behavior as they provide convincing proofs of the choice of the set of external parameters (τ, t_c, μ) in the stability region for each channel studied.

4. The interpolating operators

In the first part of the paper, we choose to work with the $\bar{3}_c 3_c$ lowest dimension interpolating currents of the four-quark states given in Table 1.

Some other choices such as $\bar{6}_c 6_c$, $\bar{8}_c 8_c$ and/or higher dimension operators used in the current literature will be checked and (critically) reviewed in the second part of the paper.

Table 1
Interpolating operators describing the Z_c, X_c, $T_{cc\bar{q}'\bar{q}}$ states discussed in this paper where $b=0$ is the optimized mixing parameter [23].

States	$I(J^P)$	$\bar{3}_c 3_c$ Four-quark currents	Refs.
Z_c	(1^+)	$\mathcal{O}_{A_{cq}} = \epsilon_{ijk}\epsilon_{mnk}[(q_i^T\, C\gamma_5\, c_j)(\bar{q}'_m\gamma_\mu C\,\bar{c}_n^T) + b, (q_i^T\, C\, c_j)(\bar{q}'_m\gamma_\mu\gamma_5 C\,\bar{c}_n^T)]$	[23]
		$\mathcal{O}_{D_q^* D_q} = (\bar{c}\gamma_\mu q)(\bar{q}'\, i\gamma_5 c)$	
X_c	(1^+)	$\mathcal{O}_X^3 = \epsilon_{ijk}\,\epsilon_{mnk}[\left(q_i^T\, C\gamma_5\, c_j\right)\left(\bar{c}_m\,\gamma^\mu C\,\bar{q}_n^T\right) + \left(q_i^T\, C\gamma^\mu\, c_j\right)\left(\bar{c}_m\,\gamma_5 C\,\bar{q}_n^T\right)]$	[18,49–51]
		$\mathcal{O}_X^6 = \epsilon_{ijk}\,\epsilon_{mnk}[\left(q_i^T\, C\gamma_5\lambda_{ij}^a\, c_j\right)\left(\bar{c}_m\,\gamma^\mu C\lambda_{mn}^a\,\bar{q}_n^T\right) + \left(q_i^T\, C\gamma^\mu\lambda_{ij}^a\, c_j\right)\left(\bar{c}_m\,\gamma_5 C\lambda_{mn}^a\,\bar{q}_n^T\right)]$	
		$\mathcal{O}_{D_q^* D_q} = \frac{1}{\sqrt{2}}[(\bar{q}\gamma_5 c)(\bar{c}\gamma_\mu q) - (\bar{q}\gamma_\mu c)(\bar{c}\gamma_5 q)]$	
		$\mathcal{O}_{\psi\pi} = (\bar{c}\gamma_\mu\lambda^a c)(\bar{q}\gamma_5\lambda^a q)$	
$T_{cc\bar{u}\bar{d}}$	$0(1^+)$	$\mathcal{O}_T^{1^+} = \frac{1}{\sqrt{2}}\epsilon_{ijk}\,\epsilon_{mnk}\left(c_i^T\, C\gamma^\mu\, c_j\right)[\left(\bar{u}_m\,\gamma_5 C\,\bar{d}_n^T\right) - \left(\bar{d}_m\,\gamma_5 C\,\bar{u}_n^T\right)]$	[50]
$T_{cc\bar{u}\bar{s}}$	$\frac{1}{2}(1^+)$	$\mathcal{O}_{T_{us}^{1^+}} = \epsilon_{ijk}\,\epsilon_{mnk}\left(c_i\, C\gamma^\mu c_j^T\right)\left(\bar{u}_m\,\gamma_5 C\bar{s}_n^T\right)$	
$T_{cc\bar{u}\bar{d}}$	$1(0^+)$	$\mathcal{O}_T^{0^+} = \frac{1}{\sqrt{2}}\epsilon_{ijk}\,\epsilon_{mnk}\left(c_i^T\, C\gamma^\mu\, c_j\right)[\left(\bar{u}_m\,\gamma_\mu C\,\bar{d}_n^T\right) + \left(\bar{d}_m\,\gamma_\mu C\,\bar{u}_n^T\right)]$	[50]
$T_{cc\bar{u}\bar{s}}$	$\frac{1}{2}(0^+)$	$\mathcal{O}_{T_{us}^{0^+}} = \epsilon_{ijk}\,\epsilon_{mnk}\left(c_i\, C\gamma_\mu c_j^T\right)\left(\bar{u}_m\,\gamma^\mu C\bar{s}_n^T\right)$	
$T_{cc\bar{s}\bar{s}}$	$0(0^+)$	$\mathcal{O}_T^{0^+} = \epsilon_{ijk}\,\epsilon_{mnk}\left(c_i\, C\gamma_\mu c_j^T\right)\left(\bar{s}_m\,\gamma^\mu C\bar{s}_n^T\right)$	

Table 2
QCD input parameters estimated from QSSR (Moments, LSR and ratios of sum rules) used here.

Parameters	Values	Sources	Refs.
$\alpha_s(M_Z)$	0.1181(16)(3)	$M_{\chi 0c,b} - M_{\eta_{c,b}}$	[52–54]
$\overline{m}_c(m_c)$ [MeV]	1266(6)	D, $B_c \oplus J/\psi$, χ_{c1}, η_c	[52,54–59]
$\overline{m}_b(m_b)$ [MeV]	4196(8)	$B_c \oplus \Upsilon$	[52,54–59]
$\hat{\mu}_q$ [MeV]	253(6)	Light	[27,60]
$\hat{m}_s$ [MeV]	114(6)	Light	[27,60]
$\kappa \equiv \langle\bar{s}s\rangle/\langle\bar{d}d\rangle$	0.74(6)	Light-Heavy	[27,60,61]
M_0^2 [GeV^2]	0.8(2)	Light-Heavy	[27,36,62–66]
$\langle\alpha_s G^2\rangle$ [GeV^4]	$6.35(35)10^{-2}$	Light-Heavy	[52,54]
$\langle g^3 G^3\rangle/\langle\alpha_s G^2\rangle$	8.2(1.0) [GeV^2]	J/ψ	[58,59]
$\rho\alpha_s\langle\bar{q}q\rangle^2$ [GeV^6]	$5.8(9)10^{-4}$	Light, τ-decay	[36,63,64,67–70]

The chiral partner 1^- and 0^- states and the molecule assignments of the $T_{QQ\bar{q}\bar{q}'}$ states which deserves a particular attention due to the numerous possibilities of such assignments are postponed in a future publication.

5. QCD input parameters

The QCD parameters which shall be used here are the QCD coupling α_s, the charm quark mass m_c, the gluon condensates $\langle\alpha_s G^2\rangle$. Their values are given in Table 2. We shall use $n_f = 4$ and 5 total number of flavours for the numerical value of $a_s \equiv \alpha_s/\pi$.

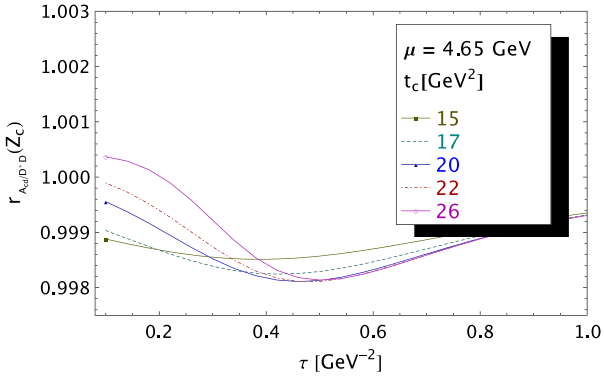

Fig. 2. $r_{A_{cd}/D*D}$ as function of τ at NLO for # values of t_c, for $\mu = 4.65$ GeV [23,24] and for the QCD inputs in Table 2.

6. The $Z_c(1^+)$ state

- Mass and decay constant from LSR

The extraction of the Z_c mass has been discussed in details in Ref. [23] using the current in Table 1 where the main source of the errors in the mass determination is the localization of the inflexion point at which the optimal value is extracted ($\Delta M = 40$ MeV) and the truncation of the OPE ($\Delta M = 39$ MeV). The results for a D^*D molecule and for a four-quark state configurations are [18,23]:

$$M_{D*D} = 3912(61)\ \text{MeV}, \qquad M_{A_{cd}} = 3889(58)\ \text{MeV}, \tag{10}$$

which are almost degenerated (we do not consider the isospin violation).

- Ratio $r_{A_{cd}/D*D}$ of masses from DRSR

We use the DRSR for studying the ratio of masses. The analysis is shown in Fig. 2. The optimal result is obtained for the sets $(\tau, t_c) = (0.46, 20)$ $(\text{GeV}^{-2}, \text{GeV}^2)$ where both present minimum. At these values, one deduces:

$$r_{A_{cd}/D*D} = 0.9981(6) \quad \Longrightarrow \quad M_{A_{cd}} = 3905(61)\ \text{MeV}, \tag{11}$$

which consolidates the previous result from a direct determination.

- $\mathcal{T}_{Z_c}$ tetramole

Noting in [23,24] that the molecule D^*D and the four-quark states are almost degenerated and have almost the same coupling to their respective current, we expect the physically observed state to be their mean which we named *tetramole* ($\mathcal{T}_{Z_c}$). One obtains:

$$M_{\mathcal{T}_{Z_c}} = 3900(42)\ \text{MeV}, \qquad f_{\mathcal{T}_{Z_c}} = 155(11)\ \text{keV}, \tag{12}$$

which coincides with the experimental $Z_c(3900)$ mass.

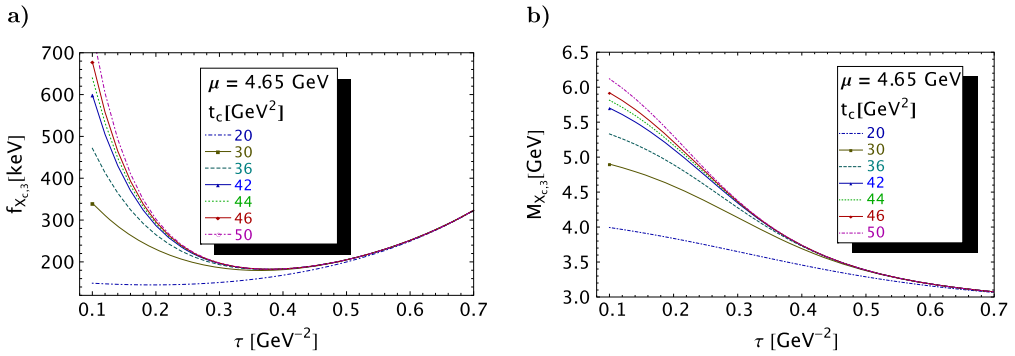

Fig. 3. $f_{X_{c,3}}$ and $M_{X_{c,3}}$ as function of τ at NLO for # values of t_c, for $\mu = 4.65$ GeV and for the QCD inputs in Table 2.

Table 3
Values of the set of LSR parameters (t_c, τ) in units of $(\text{GeV}^2, \text{GeV}^{-2} \times 10^2)$ at the optimization region for the PT series up to NLO and for the OPE truncated at the dimension-six condensates and for $\mu = 4.65$ GeV for the charm states.

X_c	$T^{1^+}_{cc}$	$T^{1^+}_{ccqs}$	$T^{0^+}_{cc}$	$T^{0^+}_{ccqs}$	$T^{0^+}_{ccss}$	$\frac{A_{cd}}{D^*D}$	$\frac{6}{3}$	$\frac{\psi\pi}{3}$	$\frac{T^{1^+}_{cc}}{X_c}$	$\frac{T^{1^+}_{ccqs}}{T^{1^+}_{ccqq}}$	$\frac{T^{0^+}_{cc}}{X_c}$	$\frac{T^{0^+}_{cc}}{T^{1^+}_{cc}}$	$\frac{T^{0^+}_{ccqs}}{T^{0^+}_{ccqq}}$	$\frac{T^{0^+}_{ccss}}{T^{0^+}_{ccqq}}$
$\mathbf{t_c}$	30–46	30–46	30–46	30–46	30–46	30–46	20	20	15–20	15–20	23–32	15–20	17–22	23–32	23–32
τ	36; 37	31; 34	32; 35	31; 34	32; 35	32; 35	46	46	132; 136	124; 130	72; 74	128; 132	50; 74	72; 74	72; 74

7. Revisiting the $X_c(1^+)$ state

- Mass and decay constant from the $\mathcal{O}^3_X$ current using LSR

The mass and coupling of the $X_c(1^+)$ have been extracted to lowest order (LO) [49–51] using the interpolating four-quark currents given in Table 1 and molecule D^*D and $J/\psi\pi$ currents given in the original papers and quoted in Table 1. These early results have been improved in [18] for the $\mathcal{O}^3_T$ current by including NLO PT corrections in order to justify the use of the running heavy quark mass of the $\overline{MS}$-scheme in the analysis. We have noticed that the localization of the inflexion point where the mass is extracted is one of the main source of the errors. We repeat the analysis of [18] here by paying attention on this choice of τ. We show the analysis in Fig. 3. Using the value of the set $(\tau, t_c) = (0.36, 30)$ to $(0.37, 46)$ $(\text{GeV}^{-2}, \text{GeV}^2)$ corresponding to the τ minimum of $f_{X_{c,3}}$ which is necessary for a better localization of the inflexion point of $M_{X_{c,3}}$, we obtain:

$$f_{X_{c,3}} = 183(16) \text{ keV}, \qquad M_{X_{c,3}} = 3876(76) \text{ MeV}, \tag{13}$$

where $f_{X_{c,3}}$ is normalized as $f_\pi = 131$ MeV. The set of (τ, t_c) used in the optimization procedure are given in Table 3. The different sources of errors are given in Table 4. One can notice the remarkable agreement of the central value of the mass with the data 3871.69(17) MeV [71].

- μ-dependence of the mass and decay constant from $\mathcal{O}^3_X$ using LSR

We show in Fig. 4 the μ-dependence of $f_{X_{c,3}}$ and $M_{X_{c,3}}$ for given values of $t_c = 46$ GeV^2 and of $\tau = 0.37$ GeV^{-2}. The optimal result is obtained at:

$$\mu_c = (4.65 \pm 0.05) \text{ GeV}, \tag{14}$$

Table 4
Sources of errors of T_{cc}, X_c and their ratios of masses. We take $|\Delta\mu| = 0.05$ GeV and $|\Delta\tau| = 0.01$ GeV^{-2}. For ratios, the errors quoted in the table are multiplied by a factor of 10^3.

Observables	Δt_c	$\Delta\tau$	$\Delta\mu$	$\Delta\alpha_s$	ΔPT	Δm_s	Δm_c	$\Delta\overline{\psi}\psi$	$\Delta\kappa$	ΔG^2	ΔM_0^2	$\Delta\overline{\psi}\psi^2$	ΔG^3	ΔOPE	ΔM_G	Values
Coupling [keV]																
f_{X_c}	1.43	0.17	0.85	4.25	0.40	···	2.49	1.67	···	0.02	1.89	7.71	0.00	10.9	5.32	183(16)
$f_{T_{cc}^{1+}}$	7.22	0.55	2.14	10.2	4.02	···	6.00	0.00	···	0.13	0.00	27.0	0.02	33.6	14.2	491(48)
$f_{T_{ccqs}^{1+}}$	4.93	0.36	1.42	6.70	3.59	0.13	4.11	0.11	8.22	0.10	0.27	16.0	0.02	20.4	8.65	317(30)
$f_{T_{cc}^{0+}}$	13.0	0.95	3.75	17.8	4.17	···	10.3	0.00	···	0.12	0.00	47.2	0.16	58.4	25.3	841(83)
$f_{T_{ccqs}^{0+}}$	8.73	0.62	2.48	11.7	3.85	0.21	7.06	0.22	14.4	0.009	0.21	28.1	0.13	35.6	14.8	542(53)
$f_{T_{ccss}^{0+}}$	14.3	0.86	3.29	15.5	4.87	0.93	9.85	0.34	34.3	0.16	0.44	32.6	0.22	41.2	33.7	718(75)
Mass [MeV]																
M_{X_c}	17.2	48.6	2.42	13.4	0.02	···	5.93	8.48	···	0.07	5.58	4.10	0.00	52.9	···	3876(76)
$M_{T_{cc}^{1+}}$	8.66	59.4	3.03	12.1	0.07	···	5.20	0.00	···	0.10	0.00	7.93	0.09	39.4	···	3885(74)
$M_{T_{ccqs}^{1+}}$	9.90	56.9	3.13	15.2	0.00	1.63	5.18	0.30	5.49	0.08	0.80	9.64	0.11	65.0	···	3940(89)
$M_{T_{cc}^{0+}}$	6.90	58.2	2.86	12.2	0.00	···	4.91	0.00	···	0.12	0.00	11.9	0.17	52.9	···	3882(81)
$M_{T_{ccqs}^{0+}}$	8.20	57.8	2.96	14.4	0.02	1.54	4.86	0.10	5.70	0.18	0.39	9.70	0.24	66.1	···	3936(90)
$M_{T_{ccss}^{0+}}$	1.00	59.0	3.04	14.8	0.01	3.61	4.65	0.02	7.17	0.26	0.73	9.10	0.36	36.2	···	4063(72)
Ratio																
r_{A_{cd}/D^*D}	0.20	0.20	0.00	0.01	0.00	···	0.03	0.06	···	0.00	0.48	0.11	0.04	0.28	···	0.9983(6)
$r_{6/3}$	0.25	0.25	0.00	0.02	0.00	···	0.05	0.08	···	0.03	0.84	0.21	0.00	0.35	···	0.9969(10)
$r_{\psi\pi/3}$	0.03	0.01	0.01	0.03	0.00	···	0.03	0.06	···	0.01	0.54	0.15	0.00	0.37	···	1.0034(7)
$r_{T_{cc}^{1+}/X_c}$	0.04	0.01	0.01	0.04	0.00	···	0.04	0.09	···	0.01	0.58	0.16	0.01	0.76	···	1.0035(10)
$r_{T_{ccqs}^{1+}/T_{ccqq}^{1+}}$	0.03	0.01	0.02	0.12	0.00	0.76	0.04	0.06	0.39	0.01	0.01	0.29	0.01	0.92	···	1.0115(13)
$r_{T_{cc}^{0+}/X_c}$	0.03	0.00	0.01	0.04	0.00	···	0.05	0.07	···	0.00	0.56	0.17	0.01	0.76	···	1.0033(10)
$r_{T_{cc}^{0+}/T_{cc}^{1+}}$	0.10	0.00	0.00	0.02	0.00	···	0.01	0.00	···	0.05	0.00	0.09	0.02	0.17	···	0.9994(2)
$r_{T_{ccqs}^{0+}/T_{ccqq}^{0+}}$	0.04	0.02	0.01	0.12	0.00	0.76	0.04	0.06	0.36	0.01	0.02	0.26	0.01	0.85	···	1.0113(12)
$r_{T_{ccss}^{0+}/T_{ccqq}^{0+}}$	0.14	0.10	0.05	0.27	0.00	1.79	0.10	0.08	0.85	0.04	0.06	0.55	0.04	1.72	···	1.0280(27)

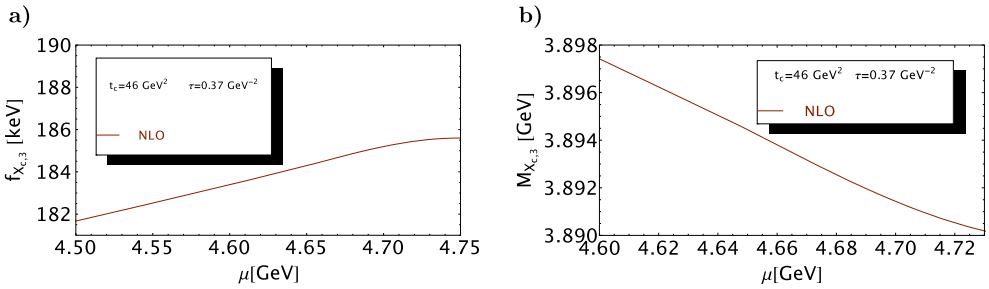

Fig. 4. $f_{X_{c,3}}$ and $M_{X_{c,3}}$ as function of μ at NLO for given values of t_c and τ for the QCD inputs in Table 2.

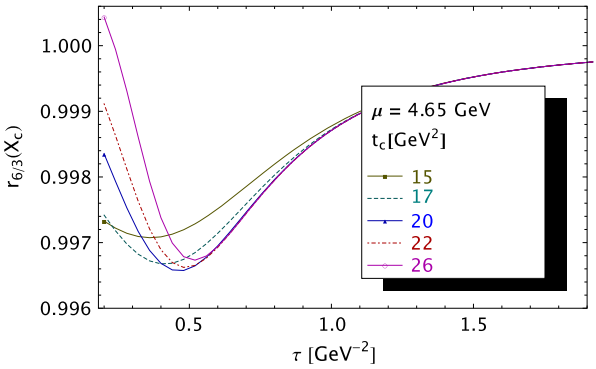

Fig. 5. $r_{6/3}$ as function of τ at NLO for # values of t_c, for $\mu = 4.65$ GeV and for the QCD inputs in Table 2.

which appears to be an (almost) universal value for the four-quark and molecule states analysis of the charm quark channels [18,22–24]. This value of μ will be used in the analysis of the charm states in the rest of the paper.

- Mass from the $\mathcal{O}_X^6$ current using DRSR

In the following, we improve the analysis in [50] by paying attention on the different sources of errors. We consider the double ratio of sum rules (DRSR) $r_{6/3}$ which we show in Fig. 5. The optimal result is obtained for the set $(\tau, t_c) = (0.46, 20)$ $(\text{GeV}^{-2}, \text{GeV}^2)$ corresponding to the minimum of τ and t_c for $r_{6/3}$. One can notice that the stability region is obtained at earlier value of t_c for the DRSR compared to the one for the LSR due to the partial cancellation of the QCD continuum contribution in the DRSR. We obtain:

$$r_{6/3} = 0.9966(10) \quad \Longrightarrow \quad M_{X_{c,6}} = 3863(76)\ \text{MeV}, \tag{15}$$

where we have used the previous predicted mass for $M_{X_{c,3}}$.

- Mass from the $\mathcal{O}_{\psi\pi}$ current using DRSR

The analysis is shown in Fig. 6. Here, the DRSR presents maximum in τ. The optimal result is obtained for the sets $(\tau, t_c) = (1.32, 15)$ and $(1.36, 20)$ in units of $(\text{GeV}^{-2}, \text{GeV}^2)$ corresponding to the region of τ maximum of $r_{\psi/3}$ and to the stability of t_c. We obtain:

$$r_{\psi\pi/3} = 1.0034(7) \quad \Longrightarrow \quad M_{X_{c,\psi\pi}} = 3889(76)\ \text{MeV}, \tag{16}$$

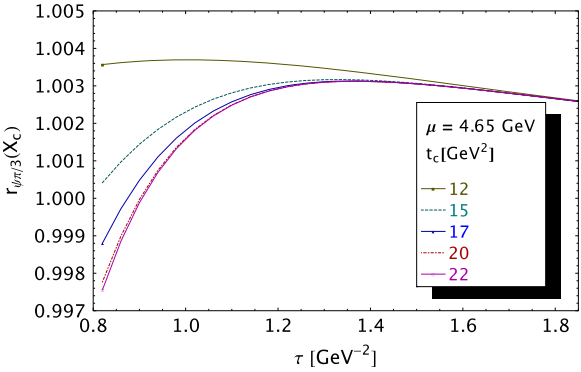

Fig. 6. $r_{\psi\pi/3}$ as function of τ at NLO for # values of t_c, for $\mu = 4.65$ GeV and for the QCD inputs in Table 2.

where we have used the previous predicted mass for $M_{X_{c,3}}$. Notice that in [50], the optimal value has been taken in a (misleading) minimum of τ where the result does not have t_c-stability.

- Mass from the $\mathcal{O}_{D^*D}$ current using DRSR

This current has been studied in Ref. [18,50,72]. Here we use the compact integrated QCD expression of the spectral function from [18] for our analysis of the DRSR $r_{D^*D/3}$. Inspecting our QCD expression of X_{c,D^*D} from [18] and the one for Z_{c,D^*D} in [23], one can deduce that in our approximation without isospin violation, ($m_u = m_d = 0$ and $\langle\bar{u}u\rangle = \langle\bar{d}d\rangle$) the two expressions are identical (isospin symmetry) such that:

$$r_{D^*D/3} = 1 \quad \Longrightarrow \quad M_{X_{c,D^*D}} = M_{Z_{c,D^*D}} = 3912(61)\ \text{MeV}. \tag{17}$$

We plan to analyze the isospin violation in a future work.

- $\mathcal{T}_{X_c}$ tetramole

Taking the fact that the different assignments to X_c lead to almost degenerated states and almost the same coupling to the currents, we consider that the observed state is their combination which we call tetramole $\mathcal{T}_{X_c}$ with the mean mass and coupling:

$$M_{\mathcal{T}_{X_c}} = 3876(44)\ \text{MeV}, \qquad f_{\mathcal{T}_{X_c}} = 183(16)\ \text{keV}. \tag{18}$$

We have not included the contribution of the D^*D molecule as it does not take into account the isospin violation.

8. Conclusion from the Z_c and X_c analysis

From the previous discussions, one can notice that the sum rules reproduce quite well the experimental masses of the $X_c(3872)$ and $Z_c(3900)$ within the molecules or/and four-quark state configurations. The DRSR has improved the accuracy of the predictions compared to the previous ones in the literature.[4]

[4] For reviews on previous LO QCD spectral sum rules results in the literature, see e.g. [73–75]. See also Ref. [76].

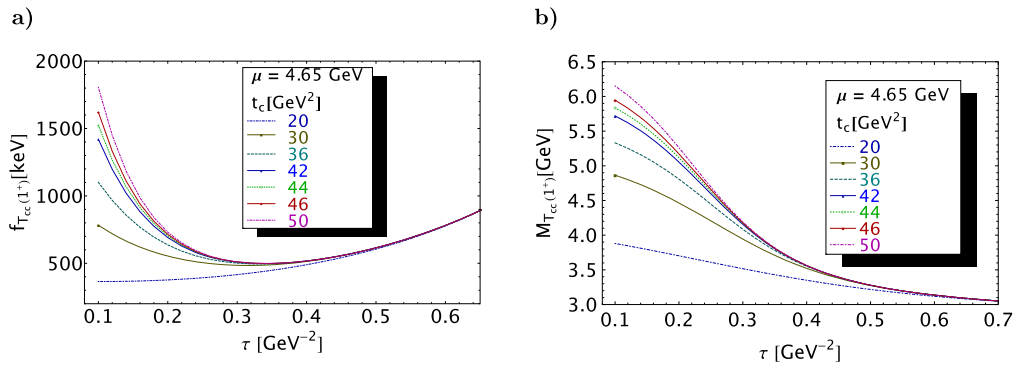

Fig. 7. $f_{T_{cc}^{0+}}$ and $M_{T_{cc}^{0+}}$ as function of τ for # values of t_c, for $\mu = 4.65$ GeV and for the QCD inputs in Table 2.

However, one can notice as in [51] that the alone study of the mass of the X_c and Z_c cannot provide a sharp selection for the four-quark and/or molecule nature of these states without studying in details their decay modes. At the present stage, we can only provide a description of these states as *tetramole* ($\mathcal{T}$) states.

Another point which deserves future studies is the careful analysis of isospin violation which can differentiate the role of D^*D, DD, ... in the molecule description of these states. We plan to come back to this point in a future work.

In the following part of the paper, we shall definitely use the experimental mass $X_c(3872)$ for a normalization of the DRSR analysis of the T_{ccqq}-like states together with the corresponding four-quark current $\mathcal{O}_X^3$ which provides the best prediction compared to the data (see Eq. (13)). Instead, we could have also choosen to work with the currents D^*D and A_{cd} which also reproduce quite well the experimental $Z_c(3900)$ mass. Unfortunately, the corresponding DRSR do not present τ-stability.

Hereafter, the $X_{c,3}$ state will be also called X_c and will be identified with the experimental $X_c(3872)$ state.

9. The $T_{cc\bar{u}\bar{d}} \equiv T_{cc}$ (1^+) state

Since, the pioneering work of [77], the mass and coupling of $T_{cc\bar{q}\bar{q}'}$ and its beauty analogue have been extracted from LSR by different groups [50,78–82]. In this paper, we improve and extend the analysis in [50] using LSR and DRSR by including the factorized NLO PT contributions and by paying more carefully attention on the different sources of the errors. In the following, we shall consider the four-quark currents given in Table 1.

- Mass and decay constant from LSR at NLO

The τ and t_c behaviors are very similar to the case of X_c and are shown in Fig. 7. The stability region (minimum in τ for the coupling and inflexion point for the mass) is obtained for the sets $(\tau, t_c) = (0.31, 30)$ to $(0.34, 46)$ in units of (GeV^{-2}, GeV^2) (see Table 3) from which we deduce:

$$f_{T_{cc}}(1^+) = 491(48)\ \text{KeV}, \qquad M_{T_{cc}}(1^+) = 3885(123)\ \text{MeV}\ , \tag{19}$$

where the mass can be compared with the experimental value $M_{T_{cc}}(1^+) = 3875$ MeV [43].

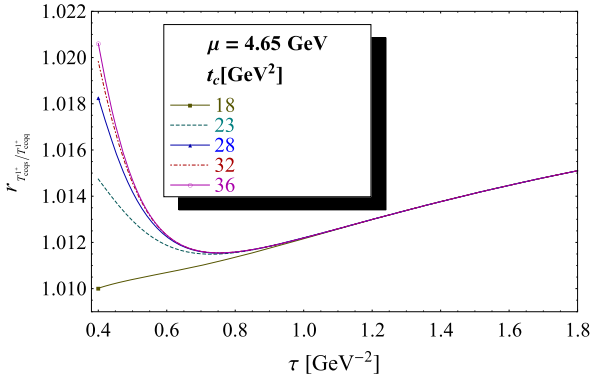

Fig. 8. $r_{T_{cc\bar{s}\bar{u}}/T_{cc}}(1^+)$ ratio of masses as function of τ at NLO for # values of t_c, for $\mu = 4.65$ GeV and for the QCD inputs in Table 2.

- Ratio of masses $r_{T_{cc}^{1+}/X_c}$ from DRSR

The result of the analysis is very similar to the one in Fig. 6. The optimal result is obtained for the sets $(\tau, t_c) = (1.24, 15)$ to $(1.30, 20)$ in units of $(\text{GeV}^{-2}, \text{GeV}^2)$ (see Table 3):

$$r_{T_{cc}^{1+}/X_c} = 1.0035(10) \quad \Longrightarrow \quad M_{T_{cc}}(1^+) = 3886(4)\ \text{MeV} \tag{20}$$

where we have taken the experimental mass of the $X_c(3872)$ [71]. The result is in perfect agreement with the direct mass determination in Eq. (19) but very accurate as the DRSR is less affected by systematics which tend to cancel out.

- Final prediction for $M_{T_{cc}}(1^+)$

As a final prediction, we take the mean of the two previous determinations and take the most precise error:

$$M_{T_{cc}}(1^+) = 3886(4)\ \text{MeV}. \tag{21}$$

This value is comparable with the recent LHCb data $T_{cc}(1^+) = 3875$ MeV which is (9 ± 4) MeV above the D^*D threshold of 3877 MeV [71].

10. The $T_{cc\bar{s}\bar{u}}(1^+)$ mass

- $r_{T_{cc\bar{s}\bar{u}}^{1+}/T_{cc}^{1+}}$ ratio of masses

We study the SU3 ratio of masses $r_{T_{cc\bar{s}\bar{u}}^{1+}/T_{cc}^{1+}}$ in Fig. 8. The optimal result is obtained for the sets $(\tau, t_c) = (0.72, 23)$ to $(0.74, 32)$ $(\text{GeV}^{-2}, \text{GeV}^2)$ at which we deduce:

$$r_{T_{cc\bar{s}\bar{u}}/T_{cc}(1^+)} = 1.0115(13) \quad \Longrightarrow \quad M_{T_{cc\bar{s}\bar{u}}}(1^+) = 3931(7)\ \text{MeV}. \tag{22}$$

- Decay constant and mass from LSR at NLO

Here, we extract directly the $T_{cc\bar{s}\bar{u}}$ coupling and mass from the LSR moments and ratio of moments. The τ and t_c-behaviors are very similar to the one in Fig. 3. The optimal result is

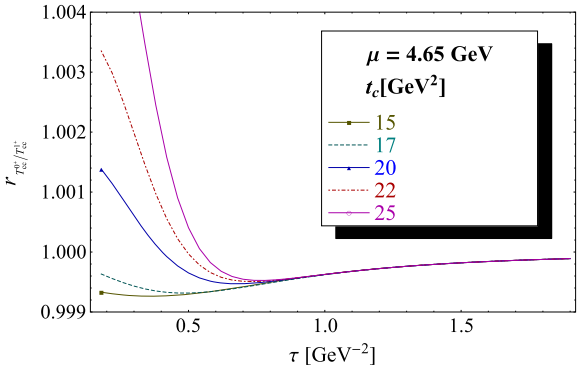

Fig. 9. $r_{T_{cc}^{0^+}/T_{cc}^{1^+}}$ as a function of τ at NLO for # values of t_c, for $\mu = 4.65$ GeV and for the QCD inputs in Table 2.

obtained for the sets $(\tau, t_c) = (0.32, 30)$ to $(0.35, 46)$ in units of $(\text{GeV}^{-2}, \text{GeV}^2)$ (see Table 3) at which the coupling presents minimum and the mass an inflexion point:

$$f_{T_{cc\bar{s}\bar{u}}}(1^+) = 317(30)\ \text{keV}, \qquad M_{T_{cc\bar{s}\bar{u}}}(1^+) = 3940(89)\ \text{MeV}\ . \tag{23}$$

- Final result

As a final result for the mass, we take the mean from the DRSR and LSR ratios:

$$M_{T_{cc\bar{s}\bar{u}}}(1^+) = 3931(7)\ \text{MeV}\ . \tag{24}$$

11. The $T_{cc\bar{u}\bar{d}}$ or T_{cc} (0^+) state

- Mass and decay constant from LSR at NLO

We pursue the analysis for the case of 0^+ state. The τ and t_c-behaviors are very similar to the ones in Fig. 3. The optimal results are obtained with the sets: $(\tau, t_c) = (0.31, 30)$ to $(0.34, 46)$ $(\text{GeV}^{-2}, \text{GeV}^2)$:

$$f_{T_{cc}}(0^+) = 841(83)\ \text{KeV}, \qquad M_{T_{cc}}(0^+) = 3882(129)\ \text{MeV}\ . \tag{25}$$

- Ratio of masses $r_{T_{cc}^{0^+}/X_c}$ from DRSR

The result of the analysis is very similar to the one in Fig. 6 from which we deduce the optimal results for the sets $(\tau, t_c) = (1.28, 15)$ to $(1.32, 20)$ $(\text{GeV}^{-2}, \text{GeV}^2)$:

$$r_{T_{cc}^{0^+}/X_c} = 1.0033(10) \quad \Longrightarrow \quad M_{T_{cc}}(0^+) = 3885(4)\ \text{MeV}, \tag{26}$$

where $X_c(3872)$ from the data has been used. The result from DRSR agrees completely with the direct determination but more accurate where the sources of the errors can be found in Table 4.

- Ratio of masses $r_{T_{cc}^{0^+}/T_{cc}^{1^+}}$ from DRSR

The result of the analysis is shown in Fig. 9 from which we deduce for the sets $(\tau, t_c) = (0.36, 15)$ to $(0.72, 20)$ $(\text{GeV}^{-2}, \text{GeV}^2)$:

$$r_{T_{cc}^{0^+}/T_{cc}^{1^+}} = 0.9994(2) \quad \Longrightarrow \quad M_{T_{cc}}(0^+) = 3878(5)\ \text{MeV}, \tag{27}$$

where we have used the mean from the $T_{cc}(1^+)$ mass predicted in Eq. (21) and the data 3875 MeV [43].

- Final value of $M_{T_{cc}^{0^+}}$ from LSR $\oplus$ DRSR

As a final value of $M_{T_{cc}^{0^+}}$, we take the mean of the previous three determinations:

$$M_{T_{cc}}(0^+) = 3883(3)\ \text{MeV}. \tag{28}$$

12. The $T_{cc\bar{s}\bar{u}}(0^+)$ mass

- $r_{T_{cc\bar{s}\bar{u}}^{0^+}/T_{cc}^{0^+}}$ ratio of masses

We study the SU3 ratio of masses $r_{T_{cc\bar{s}\bar{u}}^{0^+}/T_{cc}^{0^+}}$. The τ and t_c-behaviors are very similar to the 1^+ case in Fig. 8. The optimal result is obtained for the sets $(\tau, t_c) = (0.72, 23)$ to $(0.74, 32)$ $(\text{GeV}^{-2}, \text{GeV}^2)$ at which we deduce:

$$r_{T_{cc\bar{s}\bar{u}}/T_{cc}(0^+)} = 1.0113(12) \quad \Longrightarrow \quad M_{T_{cc\bar{s}\bar{u}}}(0^+) = 3927(6)\ \text{MeV}. \tag{29}$$

- Decay constant and mass from LSR at NLO

Here, we extract directly the $T_{cc\bar{s}\bar{u}}$ coupling and mass from the LSR moments and ratio of moments. The τ and t_c-behaviors are very similar to the ones in Fig. 3. We deduce for the sets $(\tau, t_c) = (0.32, 30)$ to $(0.35, 46)$ in units of $(\text{GeV}^{-2}, \text{GeV}^2)$ at which the coupling presents a minimum and the mass an inflexion point:

$$f_{T_{cc\bar{s}\bar{u}}}(0^+) = 542(53)\ \text{keV}, \qquad M_{T_{cc\bar{s}\bar{u}}}(0^+) = 3936(90)\ \text{MeV}\ . \tag{30}$$

- Final result

As a final result for the mass, we take the mean from the DRSR and LSR ratios:

$$M_{T_{cc\bar{s}\bar{u}}}(0^+) = 3983(7)\ \text{MeV}\ . \tag{31}$$

13. The $T_{cc\bar{s}\bar{s}}(0^+)$ state

- $r_{T_{cc\bar{s}\bar{s}}^{0^+}/T_{cc}^{0^+}}$ ratio of masses

We study the SU3 ratio of masses $r_{T_{cc\bar{s}\bar{s}}^{0^+}/T_{cc}^{0^+}}$. The τ and t_c behaviors are similar to the ones in Fig. 8. The optimal result is obtained for the sets $(\tau, t_c) = (0.72, 23)$ to $(0.74, 32)$ $(\text{GeV}^{-2}, \text{GeV}^2)$ at which we deduce:

$$r_{T_{cc\bar{s}\bar{s}}/T_{cc}(0^+)} = 1.0280(27) \quad \Longrightarrow \quad M_{T_{cc\bar{s}\bar{s}}}(0^+) = 3992(11)\ \text{MeV}. \tag{32}$$

- Decay constant and mass from LSR at NLO

Here, we extract directly the $T_{cc\bar{s}\bar{s}}$ coupling and mass from the LSR moments and ratio of moments. The τ and t_c-behaviors are very similar to the ones in Fig. 3. We deduce for the sets $(\tau, t_c) = (0.32, 30)$ to $(0.35, 40)$ in units of $(\text{GeV}^{-2}, \text{GeV}^2)$ at which the coupling presents a minimum and the mass an inflexion point:

$$f_{T_{cc\bar{s}\bar{s}}}(0^+) = 718(75)\ \text{keV}, \qquad M_{T_{cc\bar{s}\bar{s}}}(0^+) = 4063(125)\ \text{MeV}\ . \tag{33}$$

- Final result

As a final result for the mass, we take the mean from the DRSR and LSR ratios:

$$M_{T_{cc\bar{s}\bar{s}}}(0^+) = 3993(11)\ \text{MeV}\ . \tag{34}$$

We extend the previous analysis for the b-quark states

14. Z_b state

The direct determination for the molecule and four-quark assignments of the Z_b from LSR at NLO gives [24][5]:

$$f_{B^*B} = 9(2)\ \text{keV}, \qquad f_{A_{bd}} = 11(2)\ \text{MeV}, \tag{35}$$

$$M_{B^*B} = 10582(169)\ \text{MeV} \qquad M_{A_{bd}} = 10578(123)\ \text{MeV}. \tag{36}$$

The corresponding tetramole state $\mathcal{T}_{Z_b}$ has the mass and coupling:

$$M_{\mathcal{T}_{Z_b}} = 10579(99)\ \text{MeV}, \qquad f_{\mathcal{T}_{Z_b}} = 10(2)\ \text{keV}. \tag{37}$$

The mass prediction is in the range of the Belle data for $Z_b(10610)$ and $Z_b(10650)$ [83]. However, due to the large error in the mass prediction, we cannot give a sharp conclusion about the nature of these two states.

15. X_b state

We have studied this state using LSR at NLO in [18,49] (for other works see e.g. the recent reviews [73,74]). Here, we update the analysis which is shown in Fig. 10 for the four-quark current $\mathcal{O}_3$. The (τ, t_c) stabilities are obtained for $(\tau, t_c) = (0.10, 130)$ to $(0.14, 170)$ $(\text{GeV}^{-2}, \text{GeV}^2)$ where in this region, we deduce the optimal estimate:

$$f_{X_{b,3}} = 14(3)\ \text{keV}, \qquad M_{X_{b,3}} = 10545(131)\ \text{MeV}, \tag{38}$$

for a given value of $\mu = 5.2$ GeV.

We study the μ dependence of the result in Fig. 11 at NLO from which we extract an optimal value at:

$$\mu_b = (5.2 \pm 0.05)\ \text{GeV}\ . \tag{39}$$

This value of μ is (almost) universal in the b-quark channel as it is the same in all our previous works [18,22–24].

[5] For recent reviews on some other works based on QCD spectral sum rules at LO, see e.g. [73,74].

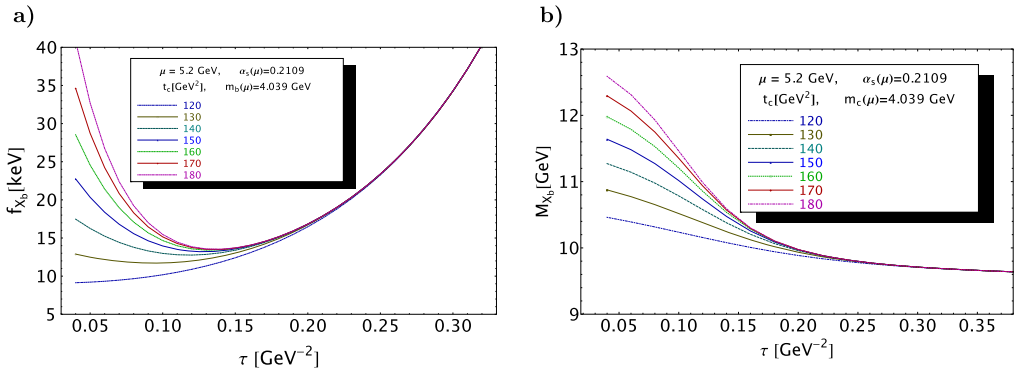

Fig. 10. $f_{X_{b,3}}$ and $M_{X_{b,3}}$ as function of τ at NLO for different values of t_c and for $\mu = 5.2$ GeV using the QCD inputs in Table 2.

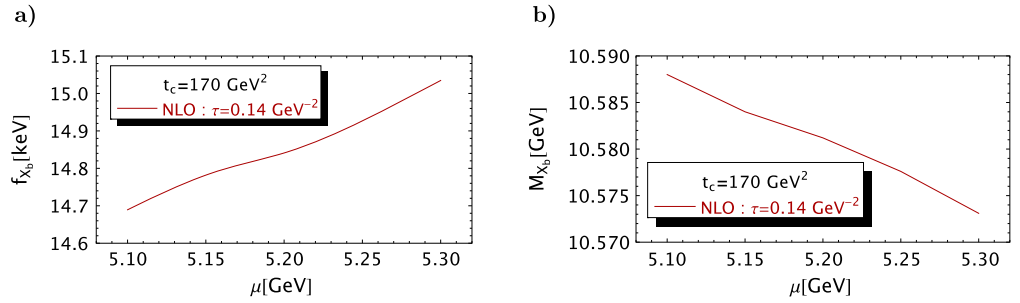

Fig. 11. $f_{X_{b,3}}$ and $M_{X_{b,3}}$ as function of μ at NLO for given values of t_c and τ for the QCD inputs in Table 2.

This result in Eq. (38) can be compared with the one in [18,49], where one can notice that the result obtained in [49] corresponds to a low range of t_c-values (104–117) GeV^2 outside the optimal region leading to a low value of $M_{X_b} = 10144(106)$ MeV. The one in Ref. [18] is 10701(172) MeV where the relatively high-central value is due to the unprecise choice of τ at the inflexion point.

One can notice that the central value of $M_{X_{b,3}}$ in Eq. (38) is below the physical B^*B threshold of 10604 MeV which goes in line with the expectations from some other approaches.[6]

16. $T_{bb}^{1^+}$ state

- $T_{bb}^{1^+}/X_b$ mass ratio from DRSR

We show the analysis of the $T_{bb}^{1^+}$ over the $X_{b,3}$ mass in Fig. 12. The optimal result is obtained for the sets: $(\tau, t_c) = (0.56, 105)$ to $(0.56, 115)$ (GeV^{-2}, GeV^2) from which we deduce:

$$r_{T_{bb}^{1^+}/3} = 1.0003(1), \qquad \Longrightarrow \qquad M_{T_{bb}^{1^+}} = 10548(131) \text{ MeV} \tag{40}$$

The sources of the errors are given in Table 6.

[6] For reviews, see e.g. [73,74,84–88,93].

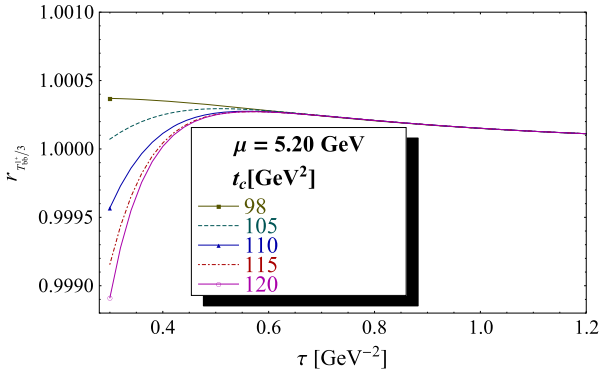

Fig. 12. $r_{T_{bb}^{1^+}/3}$ as a function of τ at NLO for # values of t_c, for $\mu = 5.2$ GeV and for the QCD inputs in Table 2.

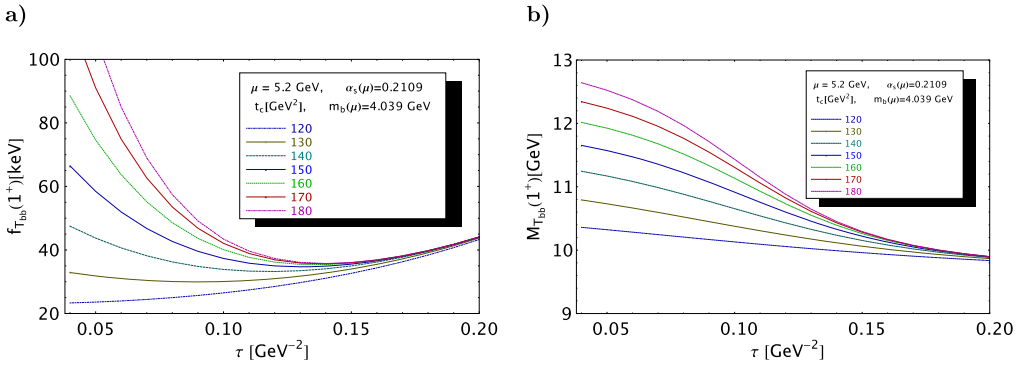

Fig. 13. $f_{T_{bb}^{1^+}}$ and $M_{T_{bb}^{1^+}}$ as function of τ for # values of t_c, for $\mu = 5.2$ GeV and for the QCD inputs in Table 2.

- Direct estimate of the $T_{bb}^{1^+}$ coupling and mass from LSR

The analysis of the $T_{bb}^{1^+}$ mass and coupling is shown in Fig. 13. The optimal result is obtained for the sets: $(\tau, t_c) = (0.09, 130)$ to $(0.14, 170)$ $(\text{GeV}^{-2}, \text{GeV}^2)$ from which we deduce:

$$f_{T_{bb}^{1^+}} = 33(7)\ \text{keV}, \qquad M_{T_{bb}^{1^+}} = 10441(147)\ \text{MeV}\ , \tag{41}$$

where the different sources of the errors are given in Table 6.

- Final result for the $T_{bb}^{1^+}$ mass

As a final result, we take the mean from the LSR and DRSR results from which we obtain:

$$M_{T_{bb}^{1^+}} = 10501(98)\ \text{MeV}\ . \tag{42}$$

17. The $T_{bb\bar{u}\bar{s}}^{1^+}$ state

- $T_{bb\bar{u}\bar{s}}^{1^+}/T_{bb}^{1^+}$ mass ratio from DRSR

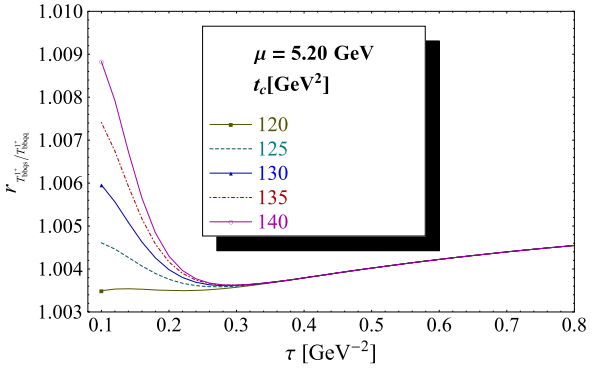

Fig. 14. $r_{T^{1^+}_{bbus}/T^{1^+}_{bb}}$ as a function of τ at NLO for # values of t_c, for $\mu = 5.2$ GeV and for the QCD inputs in Table 2.

Table 5
Values of the set of LSR parameters (t_c, τ) at the optimization region for the PT series up to NLO and for the OPE truncated at the dimension-six condensates and for $\mu = 5.20$ GeV.

	X_b	$T^{1^+}_{bb}$	$T^{1^+}_{bbqs}$	$T^{0^+}_{bb}$	$T^{0^+}_{bbqs}$	$T^{0^+}_{bbss}$	$\frac{T^{1^+}_{bb}}{X_b}$	$\frac{T^{1^+}_{bbqs}}{T^{1^+}_{bbqq}}$	$\frac{T^{0^+}_{bb}}{X_b}$	$\frac{T^{0^+}_{bb}}{T^{1^+}_{bb}}$	$\frac{T^{0^+}_{bbqs}}{T^{0^+}_{bbqq}}$	$\frac{T^{0^+}_{bbss}}{T^{0^+}_{bbqq}}$
$\mathbf{t_c}$	130–170	130–170	130–170	130–170	130–170	130–170	105–115	125–135	105–115	122	125–135	125–135
τ	10; 14	9; 14	10; 15	9; 14	10; 15	10; 15	56; 56	26; 28	58; 58	9	26; 28	26; 28

We study in Fig. 14 the SU3 breakings on the above mass ratio. The set of (τ, t_c) values $(0.26, 125)$ to $(0.28, 135)$ $(\text{GeV}^{-2}, \text{GeV}^2)$ used to get the optimal result are given in Table 5 at which we deduce:

$$r_{T^{1^+}_{bb\bar{u}\bar{s}}/T^{1^+}_{bb}} = 1.0036(3) \quad \Longrightarrow \quad M_{T^{1^+}_{bb\bar{u}\bar{s}}} = 10539(98)\ \text{MeV}, \tag{43}$$

where the value of $M_{T^{1^+}_{bb}}$ in Eq. (42) has been used.

- Direct estimate of the $T^{1^+}_{bb\bar{u}\bar{s}}$ coupling and mass from LSR

Here, we extract directly the mass and coupling of $T^{1^+}_{bb\bar{u}\bar{s}}$ from LSR. The analysis is similar to Fig. 10. The optimal result is obtained for the set of (τ, t_c) values $(0.10, 130)$ to $(0.15, 170)$ $(\text{GeV}^{-2}, \text{GeV}^2)$. We obtain:

$$f_{T^{1^+}_{bb\bar{u}\bar{s}}} = 21(4)\ \text{keV}, \qquad M_{T^{1^+}_{bb\bar{u}\bar{s}}} = 10476(153)\ \text{MeV}, \tag{44}$$

where the different sources of the errors are given in Table 6.

- Final estimate of the $T^{1^+}_{bb\bar{u}\bar{s}}$ mass

Combining the LSR and DRSR results, we deduce:

$$M_{T^{1^+}_{bb\bar{u}\bar{s}}} = 10521(83)\ \text{MeV}. \tag{45}$$

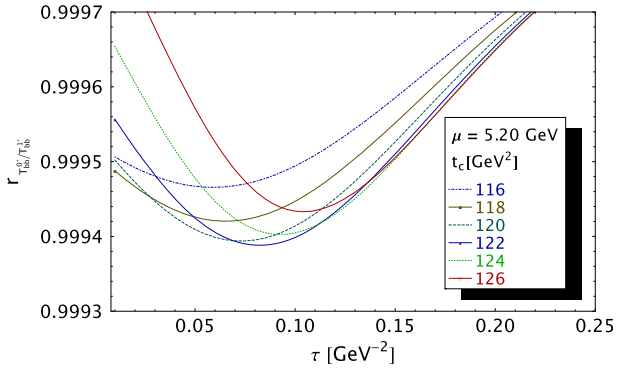

Fig. 15. $r_{T^{0^+}_{bb}/T^{1^+}_{bb}}$ as a function of τ at NLO for # values of t_c, for $\mu = 5.2$ GeV and for the QCD inputs in Table 2.

18. The $T^{0^+}_{bb}$ state

- $T^{0^+}_{bb}/X_b$ mass ratio from DRSR

The analysis of the $T^{0^+}_{bb}$ over the $X_{b,3}$ mass is similar to the 1^+ case in Fig. 12. The optimal result is obtained for the sets: $(\tau, t_c) = (0.58, 105)$ to $(0.58, 115)$ $(\text{GeV}^{-2}, \text{GeV}^2)$ from which we deduce:

$$r_{T^{0^+}_{bb}/3} = 1.0003(1), \qquad \Longrightarrow \qquad M_{T^{0^+}_{bb}} = 10501(98)\ \text{MeV}\ . \tag{46}$$

The sources of the errors are given in Table 6.

- $T^{0^+}_{bb}/T^{1^+}_{bb}$ mass ratio from DRSR

The analysis of this mass ratio is given in Fig. 15. We obtain a minimum at $\tau = 0.09$ GeV^{-2} and $t_c = 122$ GeV^2, which are in the range of the direct determinations of $M_{T^{1^+}_{bb}}$ and $M_{T^{0^+}_{bb}}$ (see Table 5). At this minimum, we deduce the optimal value:

$$r_{T^{0^+}_{bb}/T^{1^+}_{bb}} = 0.9994(1) \qquad \Longrightarrow \qquad M_{T^{0^+}_{bb}} = 10495(98)\ \text{MeV}, \tag{47}$$

after using $M_{T^{1^+}_{bb}}$ given in Eq. (42).

- Direct estimate of the $T^{0^+}_{bb}$ coupling and mass from LSR

The analysis of the $T^{0^+}_{bb}$ mass and coupling is similar to the one in Fig. 10. The optimal result is obtained for the sets: $(\tau, t_c) = (0.09, 130)$ to $(0.14, 170)$ $(\text{GeV}^{-2}, \text{GeV}^2)$ from which we deduce:

$$f_{T^{0^+}_{bb}} = 54(11)\ \text{keV}, \qquad M_{T^{0^+}_{bb}} = 10419(146)\ \text{MeV}, \tag{48}$$

where the different sources of the errors are given in Table 6.

Table 6
Sources of errors of T_{bb}, X_b and their ratios of masses. We take $|\Delta\mu| = 0.05$ GeV and $|\Delta\tau| = 0.01$ GeV^{-2}. For the ratios, the errors quoted in the table are multiplied by a factor of 10^3.

Observables	Δt_c	$\Delta\tau$	$\Delta\mu$	$\Delta\alpha_s$	ΔPT	Δm_s	Δm_c	$\Delta\overline{\psi}\psi$	$\Delta\kappa$	ΔG^2	ΔM_0^2	$\Delta\overline{\psi}\psi^2$	ΔG^3	ΔOPE	ΔM_G	Values
Coupling [keV]																
f_{X_b}	1.15	0.08	0.18	0.44	0.17	···	0.40	0.14	···	0.00	0.15	0.58	0.00	3.07	1.36	14(3)
$f_{T_{bb}^{1+}}$	2.84	0.21	0.43	0.96	0.31	···	0.61	0.00	···	0.01	0.00	1.80	0.00	3.58	4.00	33(7)
$f_{T_{bbqs}^{1+}}$	1.76	0.14	0.10	0.67	0.28	0.02	0.42	0.01	0.57	0.01	0.02	1.08	0.00	2.30	2.93	21(4)
$f_{T_{bb}^{0+}}$	4.42	0.34	0.72	1.61	0.15	···	1.00	0.00	···	0.01	0.00	3.09	0.00	6.21	6.59	54(11)
$f_{T_{bbqs}^{0+}}$	2.78	0.25	0.17	1.11	0.33	0.03	0.69	0.02	1.00	0.01	0.02	1.88	0.00	3.97	4.84	35(7)
$f_{T_{bbss}^{0+}}$	4.30	0.29	0.23	1.52	0.50	0.10	0.97	0.02	2.42	0.01	0.03	2.29	0.00	9.93	5.80	47(13)
Mass [MeV]																
M_{X_b}	26.0	115	2.92	18.7	0.55	···	14.8	8.77	···	0.20	1.48	38.9	0.00	32.0	···	10545(131)
$M_{T_{bb}^{1+}}$	9.65	119	7.40	15.4	0.26	···	7.00	0.00	···	0.13	0.00	40.0	0.00	73.8	···	10441(147)
$M_{T_{bbqs}^{1+}}$	58.9	109	2.63	16.2	0.10	2.08	7.38	0.33	20.5	0.13	0.58	60.4	0.00	59.3	···	10476(153)
$M_{T_{bb}^{0+}}$	12.6	117	7.40	15.3	0.63	···	7.10	0.00	···	0.08	0.00	39.0	0.03	74.1	···	10419(146)
$M_{T_{bbqs}^{0+}}$	61.6	108	2.58	16.1	0.10	2.05	7.48	0.30	20.3	0.05	0.30	59.9	0.05	59.7	···	10454(153)
$M_{T_{bbss}^{0+}}$	2.50	113	2.60	16.1	0.27	4.78	6.78	0.28	26.5	0.00	0.63	42.2	0.05	30.8	···	10538(129)
Ratio																
$r_{T_{bb}^{1+}/X_b}$	0.01	0.00	0.00	0.01	0.00	···	0.00	0.00	···	0.00	0.10	0.02	0.00	0.01	···	1.0003(1)
$r_{T_{bbqs}^{1+}/T_{bbqq}^{1+}}$	0.02	0.02	0.01	0.03	0.00	0.24	0.01	0.01	0.08	0.00	0.00	0.06	0.00	0.19	···	1.0036(3)
$r_{T_{bb}^{0+}/X_b}$	0.01	0.00	0.00	0.01	0.00	···	0.00	0.01	···	0.00	0.09	0.01	0.00	0.02	···	1.0003(1)
$r_{T_{bb}^{0+}/T_{bb}^{1+}}$	0.02	0.03	0.00	0.00	0.00	···	0.00	0.00	···	0.01	0.00	0.03	0.00	0.02	···	0.9994(1)
$r_{T_{bbqs}^{0+}/T_{bbqq}^{0+}}$	0.02	0.02	0.01	0.03	0.00	0.24	0.01	0.02	0.07	0.00	0.01	0.06	0.00	0.18	···	1.0035(3)
$r_{T_{bbss}^{0+}/T_{bbqq}^{0+}}$	0.06	0.01	0.02	0.07	0.00	0.56	0.02	0.02	0.14	0.01	0.01	0.11	0.01	0.75	···	1.0086(10)

- Final result for the T_{bb}^{0+} mass

As a final result, we take the mean from the three results from LSR and DRSR from which we obtain:

$$M_{T_{bb}^{0+}} = 10484(63)\ \text{MeV}\ , \tag{49}$$

where one can notice an almost degeneracy between the T_{bb} 1^+ and 0^+ masses.

19. The $T_{bb\bar{u}\bar{s}}^{0+}$ state

- $T_{bb\bar{u}\bar{s}}^{0+}/T_{bb}^{0+}$ mass ratio from DRSR

We study the SU3 breakings on the above mass ratio. The analysis is similar to Fig. 14. The sets of (τ, t_c) values used to get the optimal result are $(\tau, t_c) = (0.26, 125)$ to $(0.28, 135)$ $(\text{GeV}^{-2}, \text{GeV}^2)$ (see Table 5) at which we deduce:

$$r_{T_{bb\bar{u}\bar{s}}^{0+}/T_{bb}^{0+}} = 1.0035(3) \quad \Longrightarrow \quad M_{T_{bb\bar{u}\bar{s}}^{0+}} = 10521(63)\ \text{MeV}, \tag{50}$$

where the value of $M_{T_{bb}^{0+}}$ in Eq. (49) has been used.

- Direct estimate of the $T_{bb\bar{u}\bar{s}}^{0+}$ coupling and mass from LSR

Here, we extract directly the mass and coupling of $T_{bb\bar{u}\bar{s}}^{0+}$ from LSR. The analysis is similar to the one in Fig. 10. We obtain at $(\tau, t_c) = (0.10, 130)$ to $(0.15, 170)$ $(\text{GeV}^{-2}, \text{GeV}^2)$:

$$f_{T_{bb\bar{u}\bar{s}}^{0+}} = 35(7)\ \text{keV}, \qquad M_{T_{bb\bar{u}\bar{s}}^{0+}} = 10454(153)\ \text{MeV}, \tag{51}$$

where the different sources of the errors are given in Table 6.

- Final estimate of the $T_{bb\bar{u}\bar{s}}^{0+}$ mass

Combining the LSR and DRSR results, we deduce:

$$M_{T_{bb\bar{u}\bar{s}}^{0+}} = 10511(58)\ \text{MeV}. \tag{52}$$

20. The $T_{bb\bar{s}\bar{s}}^{0+}$ state

- $T_{bb\bar{s}\bar{s}}^{0+}/T_{bb}^{0+}$ mass ratio due to SU3 breakings from DRSR

The analysis of the $T_{bb\bar{s}\bar{s}}^{0+}$ over T_{bb}^{0+} mass is similar to Fig. 14. The SU3 breaking parameters used in the analysis are in Table 2. The optimal result is obtained for the sets: $(\tau, t_c) = (0.26, 125)$ to $(0.28, 135)$ $(\text{GeV}^{-2}, \text{GeV}^2)$ from which we deduce:

$$r_{T_{bbss}^{0+}/T_{bbqq}^{0+}} = 1.0086(10) \quad \Longrightarrow \quad M_{T_{bbss}^{0+}} = 10574(64)\ \text{MeV}\ , \tag{53}$$

where the different sources of the errors are given in Table 6.

Table 7
Summary of the results of the XZT states masses in units of MeV obtained in this paper from LSR (Tables 4 and 6) and DRSR using the currents in Table 1. Our final values are in the column "LSR ⊕ DRSR" which are the mean from LSR with the ones deduced from DRSR.

				Mass			ΔE_B	
States	J^P	Decay	Thresholds	Data	Config.	LSR	LSR ⊕ DRSR	
Z_c	1^+	$\bar{D}^0 D^{*+}$	3876	3900	D^*D	3912(61) [18,23]		
					$\bar{3}_c 3_c$	3889(58) [18,23]		
					$\mathcal{T}_{Z_c}$		*3900(42)* [18,23]	+24(42)
Z_b	1^+	$\bar{B}^0 B^{*+}$	10605		$\mathcal{T}_{Z_b}$		*10579(99)* [18,23]	−26(99)
X_c	1^+	$\bar{D}^0 D^{*+}$	3876	3872	$\bar{3}_c 3_c$	3876(76)		
					$\bar{6}_c 6_c$		3864(76)	
					$\psi\pi$		3889(76)	
					D^*D		3912(61)	
					$\mathcal{T}_{X_c}$		*3876(44)*	+0(44)
X_b	1^+	$\bar{B}^0 B^{*+}$	10605		$\bar{3}_c 3_c$	10545(131)		−60(131)
$T_{cc\bar{u}\bar{d}}$	1^+	$\bar{D}^0 D^{*+}$	3876	3875	$\bar{3}_c 3_c$	3885(74)	3886(4)	+14(4)
$T_{cc\bar{u}\bar{s}}$	1^+	$\bar{D}_s^0 D^*$	3975		–	3940(89)	3931(7)	−44(7)
$T_{cc\bar{u}\bar{d}}$	0^+	$\bar{D}^0 D^0$	3730		–	3882(81)	3883(3)	+153(3)
$T_{cc\bar{u}\bar{s}}$	0^+	$\bar{D}_s^0 D$	3833		–	3936(90)	3927(6)	+94(6)
$T_{cc\bar{s}\bar{s}}$	0^+	$D_s^+ D_s^-$	3937		–	4063(72)	3993(11)	+56(11)
$T_{bb\bar{u}\bar{d}}$	1^+	$\bar{B}^0 B^{*+}$	10605		–	10441(147)	10501(98)	−104(98)
$T_{bb\bar{u}\bar{s}}$	1^+	$\bar{B}_s^0 B^{*+}$	10692		–	10476(154)	10521(83)	−171(83)
$T_{bb\bar{u}\bar{d}}$	0^+	$\bar{B}^0 B^0$	10559		–	10419(146)	10484(63)	−75(63)
$T_{bb\bar{u}\bar{s}}$	0^+	$\bar{B}_s^0 B^0$	10646		–	10454(153)	10511(58)	−135(56)
$T_{bb\bar{s}\bar{s}}$	0^+	$\bar{B}_s^0 B_s^0$	10734		–	10538(129)	10567(57)	−167(57)

- Direct estimate of the $T^{0^+}_{bb\bar{s}\bar{s}}$ coupling and mass from LSR

The analysis of the $T^{0^+}_{bb\bar{s}\bar{s}}$ coupling and mass is similar to Fig. 10. The optimal result is obtained for the sets: $(\tau, t_c) = (0.10, 130)$ to $(0.15, 170)$ $(\text{GeV}^{-2}, \text{GeV}^2)$ from which we deduce:

$$f_{T^{0^+}_{bb\bar{s}\bar{s}}} = 47(13) \text{ keV}, \qquad M_{T^{0^+}_{bb\bar{s}\bar{s}}} = 10538(129) \text{ MeV}, \tag{54}$$

where the different sources of the errors are given in Table 6.

- Final result for the $T^{0^+}_{bb\bar{s}\bar{s}}$ mass

Combining the LSR and DRSR results, we deduce:

$$M_{T^{0^+}_{bb\bar{s}\bar{s}}} = 10567(57) \text{ MeV}. \tag{55}$$

21. General comments on the LSR results

Before comparing the different LSR results, let us address some general comments:

- Ambiguous quark mass definition at LO

As we have continuously stressed in our previous papers [17–23], the use of the running $\overline{MS}$-scheme mass in the LO expression of the spectral function is not justified as the heavy quark mass which plays a key role in the analysis is ill-defined at LO while the spectral function has been computed within the on-shell scheme where the on-shell heavy quark mass enters naturally. To that order, one can equally use the pole/on-shell quark mass. The (lucky) success of the LO results is only due to the (estimated) small NLO corrections in the $\overline{MS}$-scheme where the NLO corrections tend to compensate in the ratio of moments used to extract the ground state mass. We have demonstrated this fact in our previous papers where we have used factorization (valid to leading order in $1/N_c$) to estimate the NLO contributions [17–23]. One should note that, at this level of $(1/N_c)$ approximation for NLO, we cannot differentiate between a meson and a diquark state.

- The choice of the interpolating currents

This choice is not also trivial which may lead to inconsistencies. In the precise case of the T_{QQ} compact four-quark currents $\bar{3}_c 3_c$ used in this paper, we realize that some choices like e.g.:

$$\begin{aligned}\mathcal{O}_T^{1^+} &= \epsilon_{ijk}\,\epsilon_{mnk}\left(c_i^T\, C\gamma^\mu\, c_j\right)\left[\left(\bar{q}_m\,\gamma_5 C\,\bar{q}_n^T\right)\right.\\ &= \frac{1}{\sqrt{2}}\epsilon_{ijk}\,\epsilon_{mnk}\left(c_i^T\, C\gamma^\mu\, c_j\right)\left[\left(\bar{q}_m\,\gamma_5 C\,\bar{q'}_n^T\right)+\left(\bar{q'}_m\,\gamma_5 C\,\bar{q}_n^T\right)\right]\\ &= \cdots \end{aligned} \tag{56}$$

lead to null contributions due to SU3 symmetry.

- The QCD expressions of the two-point correlator

These expressions are non-trivial such that it is difficult to check carefully the expressions given by each author. However, in some papers, we have realized that, besides the error in the calculations, the contributions of some diagrams are missing:

– From an examination of the QCD expressions of the propagators used as inputs in the calculation, we notice that in Refs. [78–81], the propagators do not induce properly the contributions from the mixed quark-gluon $\langle\bar{q}Gq\rangle$ and gluon $\langle G^2\rangle$ condensates in Fig. 16.
– The missed diagrams also happen when the authors include high dimension operators contributions where (often) the alone contributions of some classes of diagrams are included. More drastic is the fact that some authors include $D = 8, 10, ...$ condensate contributions but (for consistency) the contribution of the $D = 6$ triple gluon condensate $\langle G^3\rangle$ is not included.
– In this and in our previous papers, we do the OPE up to $D = 6$ where ALL POSSIBLE contributions up to $D = 6$ dimension are given in integrated and compact expressions of these

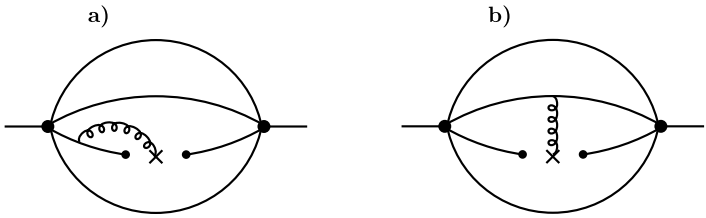

Fig. 16. Mixed quark-gluon condensate: a) self-energy; b) gluon exchange.

horrible unintegrated QCD expressions given in the literature. Such integrated expressions are easier to use.

- Values of the QCD condensates

– It is clear from the observation of the violation of the vacuum saturation for the four-quark condensates [63,64,67,69,70] and the large value of the $\langle G^3\rangle$ triple gluon condensate from charmonium sum rules [58,59] which largely deviates from the dilute gas instanton liquid model [25] that the structure and the strength of higher dimension condensates are not trivial (violation of vacuum saturation (see Table 2), mixing under renormalization [68],...). Therefore, the inclusion of only some classes of these high-dimension condensates in the OPE can be misleading. Instead, it may eventually serve as a check of the convergence of the OPE and/or an alternative estimate of the systematic errors.
– Some authors continue to use obsolete and inaccurate values of the $\langle G^2\rangle$ and $\langle G^3\rangle$ gluon condensates while the vacuum saturation to estimate the four-quark operators of dimension 6 and higher dimensions ones are used. The previous condensates have been re-estimated, as mentioned above, since the former SVZ [25] Pionner's work. The uses of different inputs are a source of discrepancy among the existing results.

- Sources of the errors

– Often, the details of the different sources of errors in the estimate are not given by the authors such that one has only to believe the errors quoted. There is not also a clear estimate of the systematic errors due to the truncation of the OPE. In our analysis and previous papers, we estimate these unknown remaining terms e.g. as:

$$\Delta\text{OPE} \approx \frac{M_Q^2\tau}{3} C_6\langle O_6\rangle, \tag{57}$$

where $C_6\langle O_6\rangle$ is the known contribution due to the dimension-six four-quark and $\langle G^3\rangle$ gluon condensates, while the factor 1/3 is the suppression factor in the LSR due to the exponential weight in the OPE. It is obvious that the OPE converges faster when the vacuum saturation is used to estimate the high-dimension vacuum condensates but the validity of a such approximation has been questioned from different phenomenological analysis from $e^+e^- \to$ hadrons, τ-decay data and baryon sum rules (see Table 2).
– In our earlier works [18–20], we have estimated the higher order terms of the PT series by an estimate of the N2LO terms. We found that these contributions are negligible.

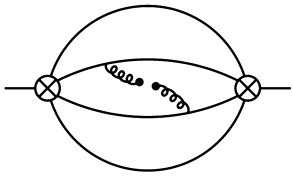

Fig. 17. Gluon condensate from one gluon exchange.

- Stability criteria

The criteria used in many papers are often ad hoc/handwavings where the per cent of the ground state and continuum contributions to the sum rules and the per cent constraint for the convergence of the OPE are fixed by hand inside the choosen *sum rule window*. On the contrary, in all our LSR works (for reviews see e.g. [27–29]) we use the optimization procedure based on the minimal sensitivity on the changes of the set (τ, t_c, μ) external variables as discussed in Section 3 which is more rigorous.

- Concluding remarks

One may say that reading some recent papers, one has the impression that the field of QCD (spectral) sum rules (QSSR) has not made any progress since its introduction by SVZ in 1979 despite the different active works done in the 80–90 for improving this nice SVZ discovery. Unfortunately, these different efforts seem to be ignored by the new generations of QCD (spectral) sum rules practitioners!

22. Checking the $T^{1^+,0^+}_{Q\bar{Q}q\bar{q}'}$ results of Wang et al. in Refs. [78,79]

Wang et al. use the same currents as in Table 1.

- QCD expressions

Comparing the QCD expressions in the 1^+ and 0^+ channels, we find that we disagree for the $\langle G^2\rangle$ gluon and mixed $\langle\bar{q}Gq\rangle$ condensates contributions while the $D=6$ $\langle G^3\rangle$ gluon condensate is missing. Inspecting the expression of the propagator, we see that the propagator used in [78, 79] does not induce the contribution of the mixed condensate shown in Fig. 16. These missed contributions for the $T_{cc\bar{u}\bar{s}}(1^+)$ state read:

$$\rho^{\langle\bar{q}Gq\rangle}_{\text{missed}}(t) = -\frac{m_Q^2 m_s\,\langle\bar{q}Gq\rangle}{3^2\times 2^5\times\pi^4}\,v\left(2+\frac{1}{x}\right)\left(1-\frac{3}{2}\right), \tag{58}$$

with: $x = m_Q^2/s$ and $v=\sqrt{1-4x}$. We also suspect that the contribution due to one gluon exchange for the $\langle G^2\rangle$ is not generated by the propagator which might explain the origin of the discrepancy. This contribution is shown in Fig. 17 and reads:

$$\rho^{\langle G^2\rangle}_{\text{missed}}(t) = -\frac{m_Q^4\langle G^2\rangle}{3^3\cdot 2^{11}\pi^6}\Big[v\Big(42x+43-88/x+3/x^2\Big)+$$

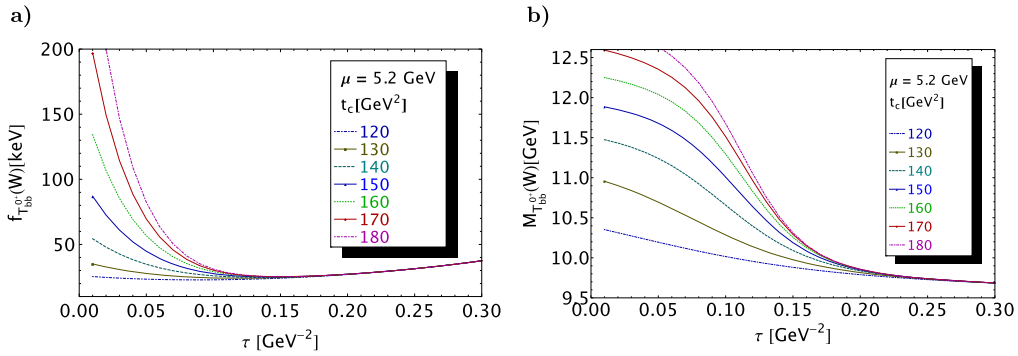

Fig. 18. $f_{T^{0+}_{bb}}$ and $M_{T^{0+}_{bb}}$ as function of τ for # values of t_c, for $\mu = 5.2$ GeV and for the QCD inputs in Table 2.

$$+6\mathcal{L}_v\Big(14x^2+12x-15+9\log(x)+8/x\Big)+108\mathcal{L}_+\Big], \tag{59}$$

with:

$$x = m_Q^2/t \ \text{ and } \ v=\sqrt{1-4x}. \tag{60}$$

Hopefully, these missed contributions do not affect in a significant way the numerical results. However, a more precise comparison cannot be done without an explicit expression of the contribution from each diagrams from the authors.

- Comparison of the mass results

– Comparing the mass results, we see a good agreement with [78] (within the errors) for the $T^{1^+,0^+}_{cc\bar{q}\bar{q}'}$ states (Fig. 24). However, one should note that the results quoted in the former paper [79] give masses higher (about 480 MeV) than the ones from [78].
– One can also note in Fig. 25, that the mass predictions for the $T^{0^+}_{bb\bar{q}\bar{q}}$ states ($q \equiv d, s$) from [79] are higher than ours by about 660 MeV. We look for the origin of this discrepancy by repeating the analysis using the (non corrected) expression of [79]. The analysis is shown in Fig. 18 where we have a nice τ stability for the coupling and an inflexion point for the mass. Both results also exhibit t_c-stability. We extract the optimal result for the set (τ, t_c) from (0.12, 130) to (0.15, 170) (GeV^{-2}, GeV^2) and deduce the central values:

$$f_{T^{0+}_{bb}} \simeq 25\,\text{keV}, \qquad M_{T^{0+}_{bb}} \simeq 10.08\,\text{GeV}, \qquad f_{T^{0+}_{bb\bar{s}\bar{s}}} \simeq 24\,\text{keV}, \qquad M_{T^{0+}_{bb\bar{s}\bar{s}}} \simeq 10.28\,\text{GeV}, \tag{61}$$

lower than the ones quoted by [79]:

$$M_{T^{0+}_{bb}} \simeq (11.14 \pm 0.16)\,\text{GeV}, \qquad M_{T^{0+}_{bb\bar{s}\bar{s}}} \simeq (11.32 \pm 0.18)\,\text{GeV}, \tag{62}$$

but in lines with our results obtained from the (corrected) QCD expression summarized in Table 7. We note that the range of t_c-values used by the authors is the same as here while the value of τ is lower in [78] explaining their overestimate of the mass result.

23. Checking the $T^{1^+}_{QQ}$ results of Agaev et al. in Ref. [80]

We see that the current used by [80] is similar to the one used in Table 1 and $\eta_5^{1^+}$ (Eq. (67)) used by [81].

- The $T_{cc}^{1^+}$ state

The QCD expression is not given by the authors. However, inspecting the form of the propagator quoted in their review paper [80], we notice that it does not also induce the diagrams in Fig. 16 while for the numerical analysis, we notice that the optimal result is obtained for the set:

$$\tau \simeq (0.17\text{–}0.25)\ \text{GeV}^{-2}, \qquad t_c \simeq (19.5\text{–}21.5)\ \text{GeV}^2, \tag{63}$$

where t_c is below the beginning of τ-stability of the coupling (Fig. 7), though the mass shows an apparent $\tau \equiv 1/M^2$ stability (in reality, it increases with M^2) in a narrow range of τ variation. As a result, the central value of the mass obtained by [80] is slightly lower than ours and the LHCb data [43]:

$$M_{T_{cc}^{1^+}} \simeq 3868(124)\ \text{MeV}, \tag{64}$$

though the errors are large.

- The $T_{bb}^{1^+}$ state

The discrepancy is more pronounced in this case where the authors extract their result using the sets:

$$\tau \simeq (0.077\text{–}0.111)\ \text{GeV}^{-2}, \qquad t_c \simeq (115\text{–}120)\ \text{GeV}^2. \tag{65}$$

Looking at Fig. 13, one can see like in the case of T_{cc} that these sets of values are outside the (true) stability region. As a result, the authors get:

$$M_{T_{bb}^{1^+}} \simeq 10035(260)\ \text{MeV}, \tag{66}$$

where the central value is much lower than ours in Table 7.

24. Checking the results of Du et al. in Ref. [81]

- The $T_{QQ\bar{q}\bar{q}}\ I(J^P) = 1(1^+)$ state

We complete the previous results from $\bar{3}_c 3_c$ currents in Table 1 by the ones from [81] where an exhaustive list is given. In particular, we shall consider as a representative for the 1^+ state the currents:

$$\begin{aligned}
\eta_1^{1^+} &\equiv \left(c_i^T\, C\gamma^\mu\, \gamma_5\, c_j\right)\left[\left(\bar{q'}_i\, C\, \bar{q}_j^T\right) + \left(\bar{q'}_i\, C\, \bar{q}_j^T\right)\right], \\
\eta_5^{1^+} &\equiv \left(c_i^T\, C\gamma^\mu\, c_j\right)\left[\left(\bar{q'}_i\, C\gamma_5\, \bar{q}_j^T\right) - \left(\bar{q'}_i\, C\gamma_5\, \bar{q}_j^T\right)\right].
\end{aligned} \tag{67}$$

(Eq. (5) of Ref. [81]) where $\eta_1^{1^+}$ gives the highest mass prediction and $\eta_5^{1^+}$ is equivalent to ours in Table 1.

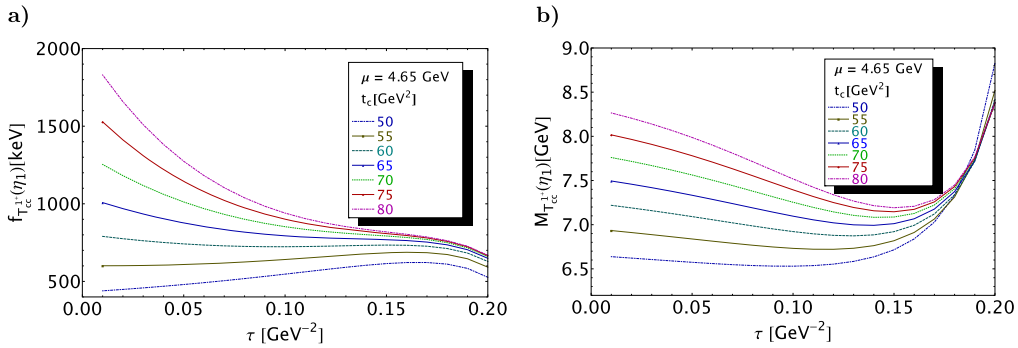

Fig. 19. $f_{T_{cc}^{1+}}$ and $M_{T_{cc}^{1+}}$ as function of τ for # values of t_c, for $\mu = 4.65$ GeV and for the QCD inputs in Table 2.

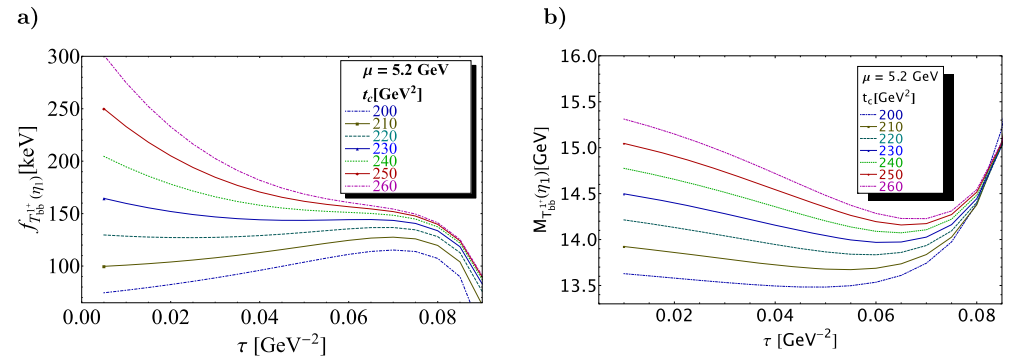

Fig. 20. $f_{T_{bb}^{1+}}$ and $M_{T_{bb}^{1+}}$ as function of τ for # values of t_c, for $\mu = 5.2$ GeV and for the QCD inputs in Table 2.

By comparing our expression for the spectral function corresponding to $\eta_5^{1^+}$ given in Appendix A with the one of [81], we notice an agreement on the PT contribution. Our expressions for the $\langle G^2\rangle$ gluon and mixed $\langle\bar{q}Gq\rangle$ condensates disagree. We notice an overall factor 3 (a misprint ?) in the four-quark contribution while the $D = 6$ $\langle G^3\rangle$ is missing.

For the $\eta_1^{1^+}$ current, our expression given in Appendix B agrees with the PT, $\langle\bar{q}q\rangle$ and four-quark condensates of [81] while there is a persisting disagreement for the $\langle G^2\rangle$ gluon and mixed $\langle\bar{q}Gq\rangle$ condensates. The $\langle G^3\rangle$ contribution is also missing.

We interpret the origin of the discrepancy for $\langle\bar{q}Gq\rangle$ as due to the expression of the propagator used in Ref. [81] which does not induce the contribution of the diagrams shown in Fig. 16.

Doing the numerical analysis, we realize that:

- The mixed quark-gluon condensate is parametrized with a wrong sign (a misprint ?).
- The choice of t_c used by the authors is too low which is outside the beginning of the true τ-stability region for the mass [$t_c \simeq 21$–28 (resp. 115–125) GeV^2] for the charm (resp. beauty) channels (see Figs. 19 and 20). Indeed, a (misleading) τ-stability is obtained for the mass but at these low values of t_c the coupling is not stable.

Using our QCD expression at NLO, we show the analysis of the T_{cc} coupling and mass in Fig. 19. We have not included the $D = 8$ contribution due to $\langle\bar{q}q\rangle\langle\bar{s}Gs\rangle$ obtained in [81]. Keeping

(consistently) the term without m_c^2 and m_c^4 in this contribution which competes with the $m_c^2\langle\bar{s}s\rangle^2$ dimension $D=6$ one, we find that it increases the mass prediction by about 40 MeV which is negligible compared to the errors of 224 MeV (see Table 8).

One can notice a (τ, t_c) stability for the sets $(0.13, 60)$ to $(0.15, 75)$ $(\text{GeV}^{-2}, \text{GeV}^2)$ for the mass which allows to fix accurately the position of the inflexion point for the coupling.

The analysis of $T_{cc\bar{s}\bar{s}}$ gives a similar behavior. An optimal result is obtained at the same sets of (τ, t_c) values. The result and the sources of the errors are given in Table 8.

Our results in this $J^P = 1^+$ channel do not support the claims of [81] on the non-existence of the T_{cc} tetraquark state.

A similar analysis is done for the T_{bb} coupling and mass which is shown in Fig. 20. The optimal results are obtained for the sets $(\tau, t_c) = (0.055, 220)$ to $(0.065, 250)$ $(\text{GeV}^{-2}, \text{GeV}^2)$. The result and the sources of the errors are given in Table 9.

One can notice that:

- The inclusion of the NLO PT corrections decreases the T_{cc} and $T_{cc\bar{s}\bar{s}}$ masses by about 188 MeV and the T_{bb} and $T_{bb\bar{s}\bar{s}}$ ones by 195 MeV.
- The SU3 breaking decreases the central value of the $T_{cc\bar{s}\bar{s}}$ by 182 MeV relative to T_{cc} and the one of $T_{bb\bar{s}\bar{s}}$ by 195 MeV relative to T_{bb}.
- Our results for the masses are definitely higher than the ones obtained in [81] despite the large errors.
- The couplings from our analysis are also large. One can understand this increases by the exponential behavior of the coupling in the LSR analysis: $f_T \sim (1/M_T^4)e^{\tau M_T^2/2}$.

- The $T_{QQ\bar{q}\bar{q}}$ $I(J^P) = 1(0^+)$ state

For this state, we use the tetraquark current given in Eq. (3) of Ref. [81]:

$$\eta_1^{0^+} = Q_i^T C Q_j \Big[\bar{q}_i C \bar{q}_j^T + \bar{q}_j C \bar{q}_i^T\Big], \quad \eta_3^{0^+} = Q_i^T C \gamma^\mu Q_j \Big[\bar{q}_i C \gamma_\mu \bar{q}_j^T - \bar{q}_j C \gamma_\mu \bar{q}_i^T\Big], \tag{68}$$

where we note that the current η_3 should give the same spectral function as the one from Table 1.

By comparing the QCD expressions for η_3, we find an agreement for the PT, $\langle\bar{q}q\rangle$ and $\langle\bar{q}q\rangle^2$ contributions but not for the $\langle G^2\rangle$ gluon and $\langle\bar{q}Gq\rangle$ mixed condensates.

A comparison of the spectral function of η_1 shows an agreement up to gluon condensate $\langle G^2\rangle$. The contribution of the mixed $\langle\bar{q}Gq\rangle$ condensate is completely different and four-quark $\langle\bar{q}q\rangle^2$ condensate differs from a minus sign.

One also notice a parametrization of the mixed condensate with a (wrong) sign (Eq. (15)) but it does not affect much the result while the (wrong) sign of the four-quark condensate changes completely the behavior of the curves and the conclusion:

> We have checked that with the wrong sign, we (almost) reproduce the result of [81] where the coupling presents a τ-stability in the region around 0.295 (resp. 0.135) GeV^{-2} and for low values $t_c \simeq 28$ (resp. 160) GeV^2 for $T^{0^+}_{cc\bar{s}\bar{s}}$ (resp. $T^{0^+}_{bb\bar{s}\bar{s}}$). We obtain at LO:

$$M_{T^{0^+}_{cc\bar{s}\bar{s}}} \simeq 4.3 \text{ GeV}, \quad f_{T^{0^+}_{cc\bar{s}\bar{s}}} \simeq 173 \text{ keV} \quad \text{and} \quad M_{T^{0^+}_{bb\bar{s}\bar{s}}} \simeq 11 \text{ GeV}, \quad f_{T^{0^+}_{bb\bar{s}\bar{s}}} \simeq 12 \text{ keV}, \tag{69}$$

Table 8
Sources of errors of the T_{cc}, T_{ccsu}, T_{ccss} couplings and masses. The PT series is known to NLO and the OPE truncated at $D = 6$ dimension condensates. We take $|\Delta\mu| = 0.05$ GeV and $|\Delta\tau| = 0.01$ GeV^{-2}. Last column: results from [81].

Observables	Δt_c	$\Delta\tau$	$\Delta\mu$	$\Delta\alpha_s$	ΔPT	Δm_s	Δm_c	$\Delta\overline{\psi}\psi$	$\Delta\kappa$	ΔG^2	ΔM_0^2	$\Delta\overline{\psi}\psi^2$	ΔG^3	ΔOPE	ΔM_G	This work	Du et al. [81]
Coupling [keV]																	
$f_{T_{cc}^{1+}}$	74.4	11.0	1.86	8.45	3.21	···	9.01	0.00	···	0.67	0.00	12.3	0.07	5.18	61.1	734(99)	···
$f_{T_{ccsu}^{1+}}$	42.9	0.86	1.36	6.20	1.20	0.41	6.47	0.56	6.29	0.52	0.19	8.01	0.06	6.61	64.3	510(103)	132
$f_{T_{ccss}^{1+}}$	45.2	7.49	2.00	9.15	1.64	1.09	9.46	3.14	13.5	0.85	0.57	11.3	0.11	7.20	50.3	710(72)	216
$f_{T_{cc}^{0+}}$	66.7	1.34	1.72	7.52	2.92	···	11.9	0.00	···	0.67	0.00	19.0	0.05	13.6	77.1	986(106)	···
$f_{T_{ccsu}^{0+}}$	35.3	0.69	1.28	4.24	3.25	0.49	11.9	0.67	6.66	0.53	0.29	14.2	0.04	7.78	54.9	677(69)	···
$f_{T_{ccss}^{0+}}$	34.9	0.72	1.89	8.33	2.75	1.23	12.3	1.73	19.8	0.84	0.84	17.2	0.07	14.4	82.8	928(96)	209
Mass [MeV]																	
$M_{T_{cc}^{1+}}$	212	12.8	0.70	2.61	1.48	···	9.57	0.00	···	1.87	0.00	62.4	0.46	32.0	···	6934(224)	···
$M_{T_{ccsu}^{1+}}$	183	11.7	0.88	3.46	1.50	1.91	9.89	2.62	33.2	2.11	1.34	62.3	0.55	34.8	···	6846(200)	4960(110)
$M_{T_{ccss}^{1+}}$	153	11.5	1.03	4.18	2.14	3.67	10.5	5.13	70.3	2.55	2.95	62.1	0.71	37.0	···	6752(184)	5030(130)
$M_{T_{cc}^{0+}}$	161	12.2	0.02	0.93	5.80	···	9.76	0.00	···	1.42	0.00	72.5	0.23	41.8	···	6758(182)	···
$M_{T_{ccsu}^{0+}}$	131	11.7	0.09	0.65	1.05	1.69	10.4	2.35	38.4	1.68	1.54	71.5	0.29	44.7	···	6650(161)	···
$M_{T_{ccss}^{0+}}$	102	10.6	0.25	0.27	0.85	3.04	10.7	4.42	79.4	1.93	3.24	71.9	0.35	50.1	···	6532(157)	5050(150)

Table 9
Same as in Table 8 but for the T_{bb}, T_{bbs}, T_{bbss} couplings and masses.

Observables	Δt_c	$\Delta\tau$	$\Delta\mu$	$\Delta\alpha_s$	ΔPT	Δm_s	Δm_c	$\Delta\overline{\psi}\psi$	$\Delta\kappa$	ΔG^2	ΔM_0^2	$\Delta\overline{\psi}\psi^2$	ΔG^3	ΔOPE	ΔM_G	This work	Du et al. [81]
Coupling [keV]																	
$f_{T_{bb}^{1+}}$	15.4	1.09	0.33	2.41	0.26	···	1.99	0.00	···	0.04	0.00	2.37	0.00	1.78	17.2	144(24)	···
$f_{T_{bbsu}^{1+}}$	6.69	0.92	0.26	1.94	0.00	0.07	1.63	0.10	0.74	0.05	0.03	1.42	0.01	5.94	16.9	112(19)	12
$f_{T_{bbss}^{1+}}$	9.46	0.75	0.33	2.40	0.07	0.89	1.97	0.20	1.77	0.06	0.07	2.12	0.01	1.24	21.0	132(24)	23
$f_{T_{bb}^{0+}}$	7.42	1.33	0.39	3.16	0.39	···	3.23	0.00	···	0.05	0.00	4.58	0.00	2.61	35.2	217(37)	···
$f_{T_{bbsu}^{0+}}$	3.54	3.63	0.27	2.17	0.10	0.07	2.20	0.10	1.28	0.04	0.05	2.85	0.00	1.88	23.9	141(25)	···
$f_{T_{bbss}^{0+}}$	3.28	0.83	0.37	2.96	0.10	0.16	2.95	0.24	3.87	0.06	0.13	3.45	0.00	2.57	31.8	181(33)	21
Mass [MeV]																	
$M_{T_{bb}^{1+}}$	243	76.3	0.70	6.90	0.79	···	9.23	0.00	···	0.78	0.00	60.6	0.13	63.2	···	14068(270)	···
$M_{T_{bbsu}^{1+}}$	199	135	0.73	7.83	0.84	2.15	12.0	3.00	41.8	1.28	1.58	73.4	0.23	88.8	···	13960(270)	10700(300)
$M_{T_{bbss}^{1+}}$	185	79.2	0.88	8.20	1.11	3.10	10.5	4.48	69.5	1.20	2.50	61.4	0.02	74.7	···	13732(234)	11000(300)
$M_{T_{bb}^{0+}}$	125	90.3	0.08	4.90	0.17	···	12.4	0.00	···	0.73	0.00	85.9	0.05	115	···	13647(211)	···
$M_{T_{bbsu}^{0+}}$	92.6	99.0	0.75	5.55	0.06	1.53	12.7	2.15	43.2	0.85	1.60	84.7	0.05	118	···	13511(206)	···
$M_{T_{bbss}^{0+}}$	71.1	87.2	0.88	6.23	0.63	2.45	13.0	3.98	91.7	0.98	3.28	83.3	0.08	109	···	13369(200)	11000(200)

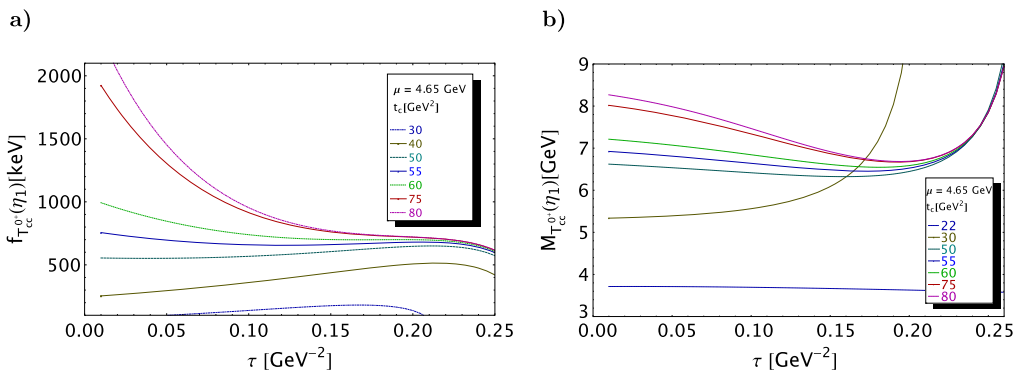

Fig. 21. $f_{T^{0+}_{cc}}$ and $M_{T^{0+}_{cc}}$ as function of τ for # values of t_c, for $\mu = 4.65$ GeV and for the QCD inputs in Table 2.

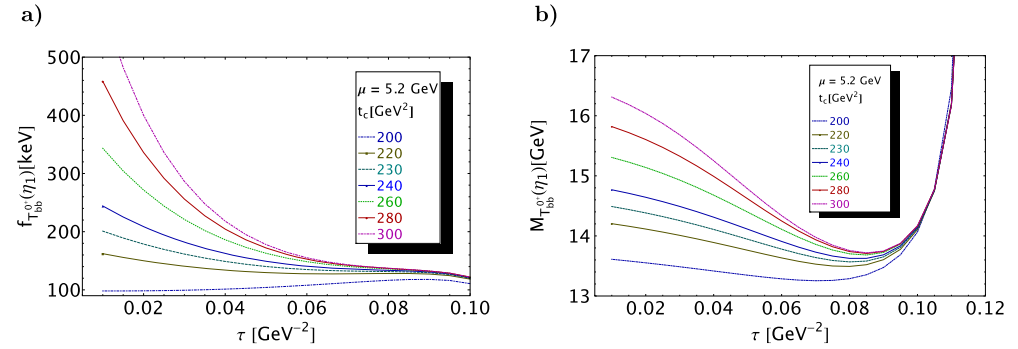

Fig. 22. $f_{T^{0+}_{bb}}$ and $M_{T^{0+}_{bb}}$ as function of τ for # values of t_c, for $\mu = 5.2$ GeV and for the QCD inputs in Table 2.

For the corrected sign, we illustrate, in Figs. 21 and 22, the analysis in the chiral limit where one can notice that the optimal results are obtained at larger values of t_c implying by duality larger values of the meson masses. Our results are summarized in Tables 8 and 9 where we conclude that the masses of $T_{QQ\bar{q}'\bar{q}}$ states associated to the η_1 current are large and can be confused with the continuum.

Our results in this $J^P = 0^+$ channel do not support the claims of [81] on the non-existence of the T_{cc} and $T_{cc\bar{s}\bar{u}}$ tetraquark states.

25. $T_{QQ\bar{q}\bar{q}'}$ state from the $\bar{8}_c 8_c$ current [82]

Here, we check the results of [82] for the molecule state built from the octet $\bar{Q}\lambda_a q$ meson. We consider, for instance, the interpolating current (Eq. (3) of [82]):

$$\mathcal{O}^{8,\mu}_{T,1} = (\bar{Q}_j \gamma^\mu \frac{\lambda_a^{jk}}{2} s_k)(Q_m\, i\gamma_5 \frac{\lambda_a^{mn}}{2} \bar{q}_n). \tag{70}$$

Notice that a similar octet current has been used for testing the 4-quark nature of the a_0 light meson [11] and of the X state [51]. Comparing our results with Ref. [82], we found that:

– The input quark propagators used in their Eqs. (7) and (8) are correct except for the $\langle G^3\rangle$ condensate contribution which is incomplete.

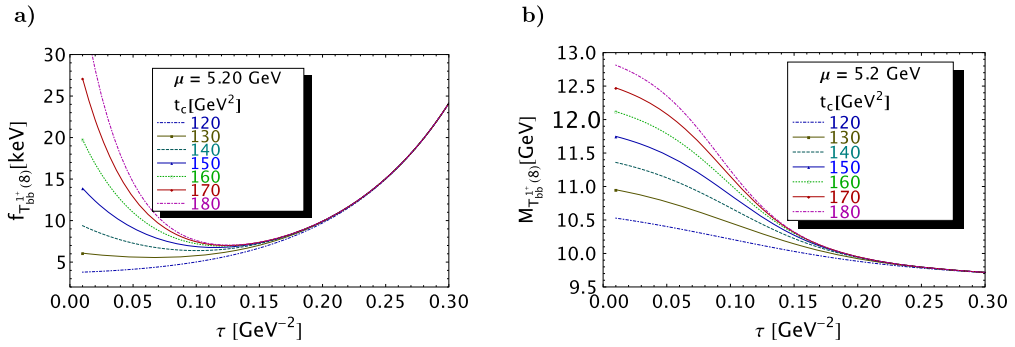

Fig. 23. $f_{T^{0+}_{bb}}$ and $M_{T^{0+}_{bb}}$ as function of τ for # values of t_c, for $\mu = 5.2$ GeV and for the QCD inputs in Table 2.

– The contribution coming from the trace for all 4 quark propagators in the spectral function is absent in Ref. [82] as well as the contribution from the $\langle \bar{q}' q' \rangle$ condensate.

We show the analysis in Fig. 23 in the case of T_{bb} and using the expression in Appendix C:

– The choice of the set $(\tau, t_c) = (0.08\text{–}0.11, 12)$ $(\text{GeV}^{-2}, \text{GeV}^2)$ used by [82] for $T^{1^+}_{bb}$ is just at the beginning of the stability region (see Fig. 23).
– Working with the spectral function of [82] and the one in Appendix C, the difference between the QCD expressions induces a small change of about 80 MeV when using the same QCD inputs. The contribution of the $\langle G^3 \rangle$ condensate is negligible as well as of the $D = 8, 10$ condensates used in [82]. However, the implicit use of factorization for the four-quark condensate increases the central value of the mass predictions by (815–829) MeV for $M_{T^{1+}_{cc\bar{q}'\bar{q}}}$ and about (590–650) MeV for $M_{T^{1+}_{bb\bar{q}'\bar{q}}}$.
– The difference between the values of the couplings can be understood by its sum rule behavior: $f_T \sim (1/M_T^4) e^{\tau M_T^2/2}$ which introduces a suppression factor of about 0.5 on our results.

From the analysis in Fig. 23, we deduce the results quoted in Table 10.

26. Comparison of different LSR results

- Results

We compare the different published LSR results in Figs. 24 and 25 for the $T^{1^+}_{QQ}$ and $T^{0^+}_{QQ}$ states. The quoted results come from the original works. However, from our previous checks, we have realized that results from [78–81] are not exactly correct which explain the divergence of some results.

- QCD expressions of the spectral function

For the QCD expressions of the spectral function, we notice that the propagator used in [78–81] does not generate the diagrams in Fig. 16 which induces a different result for the mixed

Table 10
Sources of errors and estimates of the masses and couplings of the $T^{1^+}_{QQ}$ and $T^{1^+}_{QQsu}$ ($Q \equiv c, b$) states for the $\bar{8}_c 8_c$ currents. We take $|\Delta\mu| = 0.05$ GeV and $|\Delta\tau| = 0.01$ GeV^{-2}.

Observables	Δt_c	$\Delta\tau$	$\Delta\mu$	$\Delta\alpha_s$	ΔPT	Δm_s	Δm_Q	$\Delta\overline{\psi}\psi$	$\Delta\kappa$	ΔG^2	ΔM_0^2	$\Delta\overline{\psi}\psi^2$	ΔG^3	ΔOPE	ΔM_G	This work	Ref. [82]
Coupling [keV]																	
$f_{T^{1^+}_{cc}}$	6.00	0.06	0.36	1.70	0.14	···	0.98	0.79	···	0.02	1.02	3.08	···	3.63	0.74	76(8)	···
$f_{T^{1^+}_{ccsu}}$	5.33	0.07	0.29	1.55	0.03	0.03	0.84	0.84	1.72	0.02	1.08	2.54	···	4.60	1.18	64(8)	···
$f_{T^{1^+}_{bb}}$	0.73	0.04	0.03	0.19	0.03	···	0.11	0.08	···	0.00	0.07	0.25	···	0.24	0.58	7(1)	18(1)
$f_{T^{1^+}_{bbsu}}$	0.66	0.04	0.03	0.51	0.01	0.00	0.10	0.08	0.14	0.00	0.08	0.21	···	0.78	0.53	6(1)	20(6)
Mass [MeV]																	
$M_{T^{1^+}_{cc}}$	6.79	40.9	2.09	5.93	0.07	···	4.25	5.95	···	0.11	4.40	3.62	···	42.3	···	3905(60)	4720(130)
$M_{T^{1^+}_{ccsu}}$	7.68	39.8	5.18	13.9	0.03	2.66	4.16	13.8	18.8	0.14	6.41	13.6	···	95.1	···	3931(108)	4760(140)
$M_{T^{1^+}_{bb}}$	8.60	115	1.80	11.8	0.02	···	6.65	7.58	···	0.05	3.78	17.3	···	67.7	···	10690(136)	11280(150)
$M_{T^{1^+}_{bbsu}}$	2.50	109	1.93	12.3	0.00	1.88	6.75	7.13	15.7	0.05	6.05	16.8	···	53.0	···	10706(125)	11360(160)

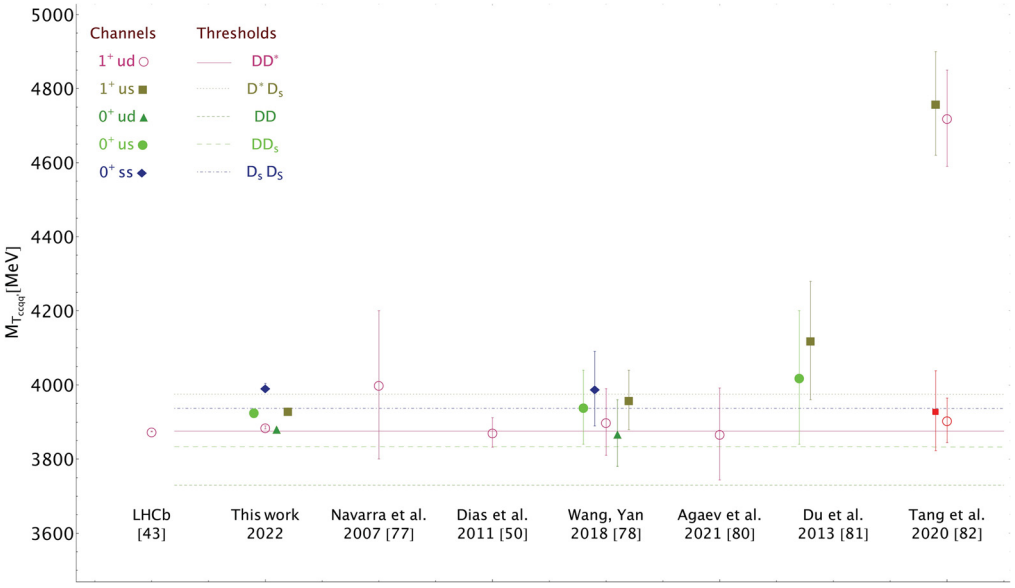

Fig. 24. Different determinations of $T_{ccqq'}^{1^+,0^+}$ from LSR. The horizontal lines are physical thresholds. Comments and corrections of some results are given in the text. The predictions of Du et al. and ours for the η_1 current quoted in Table 8 are too high and are not shown here. The red rectangle and open circle below the ones of Tang et al. are our predictions for the same $\bar{8}_c 8_c$ current. (For interpretation of the colors in the figure(s), the reader is referred to the web version of this article.)

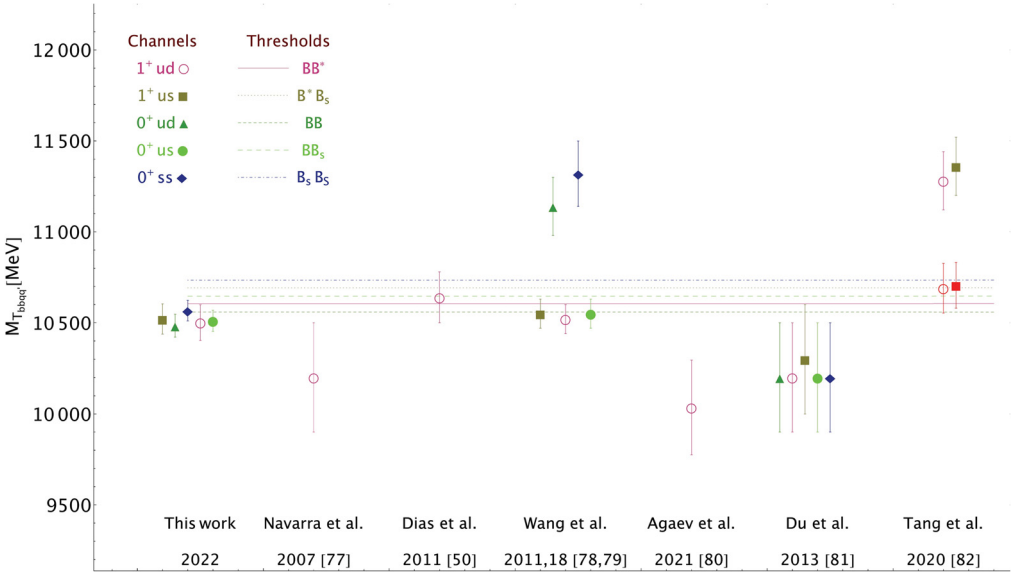

Fig. 25. Same as Fig. 24 but for $T_{bbqq'}^{1^+,0^+}$.

$\langle\bar{q}Gq\rangle$ condensate. A discrepancy is also noticed for the contribution of the gluon condensate $\langle G^2\rangle$ from the diagram in Fig. 17 while the contribution of the $\langle G^3\rangle$ condensate is often missing. Inconsistently some authors include the contribution of some classes of high-dimension condensates.

We could not (unfortunately) check the QCD expression of the spectral function used in [80] which is not given.

For Ref. [81], where many configurations are considered, we only quote the (uncorrected) lowest masses given in their Tables from the currents η_5 for the 1^+ and η_3 for 0^+ which are similar to our currents in Table 1. The (corrected) predictions from the η_1 current are given in Tables 8 and 9 but not in Figs. 24 and 25 because the mesons masses are too high.

- Concluding remarks

Despite the previous caveats on the QCD expressions and on the choice of sum rule windows, one may conclude that (within the errors):

There are (almost) good agreements among different determinations and with the data for the 1^+ $T_{cc\bar{q}\bar{q}'}$ states from the $\bar{3}_c3_c$ interpolating currents. Most of the approaches predict the T_{bb} states to be below the hadronic thresholds.
The 0^+ T_{bb} and 0^+ $T_{bb\bar{s}\bar{s}}$ states [79] predicted at relatively high masses using $\bar{3}_c3_c$ currents were quite surprising compared to the charm analogue. We have corrected these predictions in Section 22.
The predictions of [80] are usually lower than the other ones due to the fact that the authors extract the mass at lower values of t_c outside the τ-stability of the coupling. The corrected values are given in our predictions in Table 7.
The high-value of the masses from the η_3, η_5 currents quoted by [81] shown in Fig. 24 are due to the wrong sign of the four-quark condensate contribution. The corrected results are given in Tables 8 and 9. Ours do not also support the argument of [81] for the non-existence of the $1^+, 0^+$ T_{cc} and 0^+ $T_{cc\bar{s}\bar{u}}$ states.
The high central values of the masses obtained by [82] shown in Figs. 24 and 25 from the $\bar{8}_c8_c$ current are essentially due to the implicit use of four-quark condensate factorization. Results not using this assumption are given in Table 10 which go in lines with the other ones from $\bar{3}_c3_c$ current. A such conclusion is somewhat expected if one looks at the result for X in Ref. [51] where $\bar{8}_c8_c$ and $\bar{3}_c3_c$ current has been also used.

27. LSR ⊕ DRSR confronted to some other approaches

- Comparison of different results

In Fig. 26, we confront our results from LSR ⊕ DRSR with the ones from different approaches in the literature (lattice calculations [89–92], light front holographic [93], quark and potential models ⊕ heavy quark symmetry [94–96,98–103]). We refrain to comment on the technical details of the estimates from different approaches being non-experts in these fields. However, for a more meaningful comparison, we regret that most of the predictions from quark and potential models ⊕ heavy quark symmetry are quoted without any estimated errors.

One can notice from Fig. 26, that there is (almost) a consensus for the predictions of the axial-vector 1^+ masses from different approaches: the T_{cc} state is expected to be around the physical

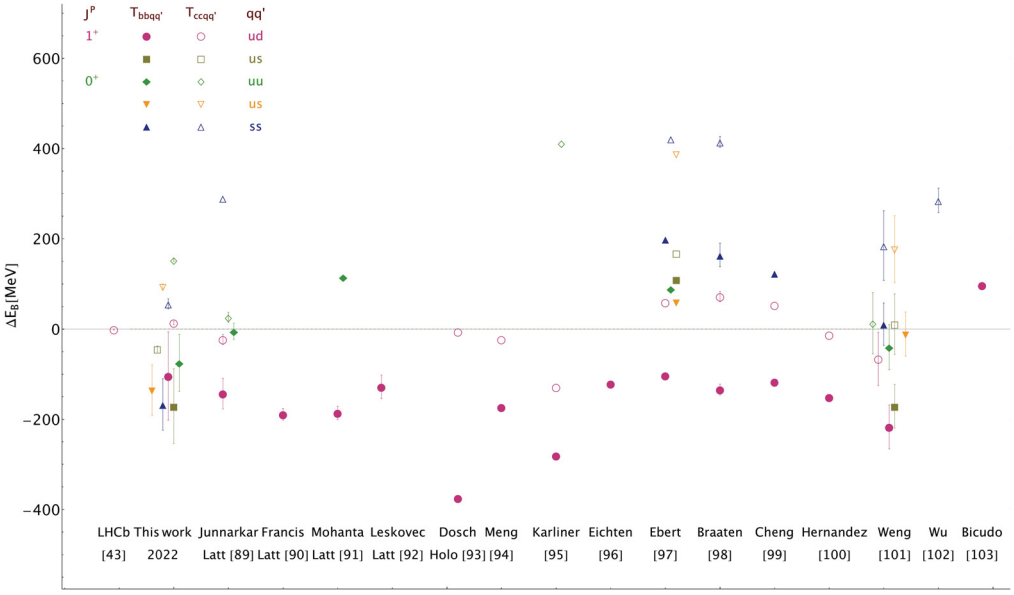

Fig. 26. Confronting the LSR ⊕ DSR results of $T^{1^+,0^+}_{QQqq'}$ masses with some estimates from lattice and quark models.

threshold while the T_{bb} one is below the threshold (except the one from [103]) and then stable against strong interactions. However, the recent LHCb data for the 1^+ T_{cc} candidate does not favor the models of [97–99] which predict a too high 1^+ T_{cc} mass.

For the T_{bb} 0^+ scalar state, the situation is quite similar. This state is expected to be below the hadronic threshold by different approaches except the lattice result of [91] and the quark model of [97].

- Some comments on our results

Our predictions for different 1^+ and 0^+ states including SU3 breakings states are clustered in the range -250 to $+150$ MeV of the hadronic thresholds.

From our approach, the mass shifts due to SU3 breakings are positive but tiny. Therefore, our results for the masses of different states are grouped around the physical thresholds. This is not often the case of some other approaches. In particular, a lattice calculation [89] and some quark models [97–99,101–103] expect a mass of the $T_{cc\bar{s}\bar{s}}$ and $T_{bb\bar{s}\bar{s}}$ 0^+ states well above the physical threshold while in our case the $T_{bb\bar{s}\bar{s}}$ state lies below the physical threshold and the one of the $T_{cc\bar{s}\bar{s}}$ 0^+ state is slightly above (see Table 5). This peculiar feature of SU3 breakings for exotic states needs to be checked experimentally.

Declaration of competing interest

The authors declare that they have no known competing financial interests or personal relationships that could have appeared to influence the work reported in this paper.

Appendix A. Spectral functions corresponding to the currents in Table 1

In this appendix,[7] we shall give the compact integrated QCD expressions of the spectral functions of the $T_{QQ\bar{q}\bar{q}'}$ states associated to the interpolating currents given in Table 1. Compared to the existing non-integrated ones given in the current literature, our expressions are more compact, less horrible and easier to handle in the numerical analysis. Checks of some existing expressions in the literature have been discussed in Section 24 and given in Appendix B.

We shall define

$$\mathcal{L}_v = \text{Log}\left[\frac{1+v}{1-v}\right], \text{ and } \rho(t) \equiv \frac{1}{\pi}\text{Im}\,\Pi(t) \text{ (see Eq. (2))}, \tag{A.1}$$

where x and $v = \sqrt{1-x}$ have been defined in Eq. (60). We use the short-handed notations:

$$\langle G^2\rangle \equiv \langle g^2 G^{\mu\nu}_a G^a_{\mu\nu}\rangle, \quad \langle\bar{q}Gq\rangle \equiv g\langle\bar{q}G^{\mu\nu}(\lambda_a/2)q\rangle, \quad \langle G^3\rangle \equiv \langle g^3 f_{abc} G^{a,\mu\nu} G^b_{\nu\rho} G^{c,\rho}_{\mu}\rangle. \tag{A.2}$$

- $T_{QQ\bar{u}\bar{q}}$ or $T_{QQ\bar{u}\bar{s}}$: $J^P = 1^+$

Its spectral function is associated to the current $\mathcal{O}_{T^{1^+}_{QQuq}}$: $q \equiv d, s$, $Q \equiv c, b$ (see Table 1). We keep the m_q-linear mass term corrections.

$$\begin{aligned}
\rho^{pert}(t) &= \frac{m_Q^8}{5\cdot 3^2\cdot 2^{12}\pi^6}\Big[v\Big(840x + 7340 + 52528/x + 5796/x^2 - 62/x^3 + 5/x^4\Big) + \\
&+120\mathcal{L}_v\Big(14x^2 + 120x + 207 - 18(9+4/x)\log(x) - 320/x - 15/x^2\Big) + \\
&-4320\mathcal{L}_+\Big(9 + 4/x\Big)\Big], \\
\rho^{\langle\bar{q}q\rangle}(t) &= \frac{m_q m_Q^4}{3\cdot 2^8\pi^4}\Big(\langle\bar{q}q\rangle - 2\langle\bar{u}u\rangle\Big)\Big[v\Big(12x + 50 - 2/x + 3/x^2\Big) \\
&+24\mathcal{L}_v\Big(x^2 + 4x - 3\Big)\Big], \\
\rho^{\langle G^2\rangle}(t) &= \frac{m_Q^4\langle G^2\rangle}{3^3\cdot 2^{11}\pi^6}\Big[v\Big(102x + 557 + 538/x + 18/x^2\Big) \\
&+6\mathcal{L}_v\Big(34x^2 + 180x - 123 - 63\log(x) - 44/x\Big) - 756\mathcal{L}_+\Big], \\
\rho^{\langle\bar{q}Gq\rangle}(t) &= \frac{m_q m_Q^2}{3^2\cdot 2^6\pi^4}\Big(\langle\bar{q}Gq\rangle + 6\langle\bar{u}Gu\rangle\Big)\,v\Big(2 + 1/x\Big), \\
\rho^{\langle\bar{q}q\rangle^2}(t) &= \frac{m_Q^2\langle\bar{u}u\rangle\langle\bar{s}s\rangle}{18\pi^2}\,v\Big(2 + 1/x\Big),
\end{aligned}$$

[7] For the X and Z states, we have used the expressions of the spectral functions given respectively in [23] and [18,49–51] which will not be reported here.

$$\rho^{\langle G^3\rangle}(t)=\frac{m_Q^2\langle G^3\rangle}{5\cdot 3^5\cdot 2^{12}\pi^6}\Big[v\Big(4020x-19490-21070/x-495/x^2+$$
$$+36m_c^2\tau(5/x^3+58/x^2)\Big)+24\mathcal{L}_v\Big(335x^2-1680x+945+$$
$$+60(6+1/x)\log(x)+440/x-18m_c^2\tau(1/x+3/x^2)\Big)+$$
$$+2880\mathcal{L}_+\Big(6+1/x\Big)\Big].$$

- $T_{QQ\bar{s}\bar{s}}$: $J^{PC}=1^+$

We note that its spectral function is identically zero.

- $T_{QQ\bar{q}\bar{q}}$: $J^P=0^+$

Its spectral function is associated to the current $\mathcal{O}_{T^{0^+}_{QQ\bar{u}\bar{d}}}$ or $\mathcal{O}_{T^{0^+}_{QQ\bar{s}\bar{s}}}$: $q\equiv u,d,s$, $Q\equiv c,b$ (see Table 1).

$$\rho^{pert}(t)=\frac{m_Q^8}{5\cdot 3\cdot 2^8\,\pi^6}\Big[v\Big(1080+5400/x+306/x^2-28/x^3+1/x^4\Big)+$$
$$+120\mathcal{L}_v\Big(18x+15-6(3+1/x)\log(x)-32/x\Big)-1440\mathcal{L}_+\Big(3+1/x\Big)\Big],$$
$$\rho^{\langle\bar{q}q\rangle}(t)=-\frac{3m_qm_Q^4\langle\bar{q}q\rangle}{4\pi^4}\Big[v\Big(2+1/x\Big)+4\mathcal{L}_v\Big(x-1\Big)\Big],$$
$$\rho^{\langle G^2\rangle}(t)=\frac{m_Q^4\langle G^2\rangle}{3\cdot 2^8\pi^6}\Big[v\Big(6+17/x+1/x^2\Big)+12\mathcal{L}_v\Big(x-\log(x)-1/x\Big)-24\mathcal{L}_+\Big],$$
$$\rho^{\langle\bar{q}Gq\rangle}(t)=\frac{m_qm_Q^2\langle\bar{q}Gq\rangle}{3\cdot 2^3\,\pi^4}\Big[v\Big(8+1/x\Big)+3\mathcal{L}_v\Big(2x-1\Big)\Big],$$
$$\rho^{\langle\bar{q}q\rangle^2}(t)=\frac{m_Q^2\langle\bar{q}q\rangle^2}{3\pi^2}\,v\Big(2+1/x\Big),$$
$$\rho^{\langle G^3\rangle}(t)=\frac{m_Q^2\langle G^3\rangle}{5\cdot 3^2\cdot 2^8\pi^6}\Big[v\Big(310+415/x-6/x^2+2m_c^2\tau(1/x^3+8/x^2)\Big)+$$
$$+4\mathcal{L}_v\Big(155x-53-10(6+1/x)\log(x)-55/x-3m_c^2\tau/x^2\Big)-$$
$$-80\mathcal{L}_+\Big(6+1/x\Big)\Big].$$

- $T_{QQ\bar{u}\bar{s}}$: $J^P=0^+$

Its spectral function is associated to the current $\mathcal{O}_{T^{0^+}_{QQ\bar{u}\bar{s}}}$ (see Table 1).

$$\rho^{pert}(t)=\frac{m_Q^8}{5\cdot 3\cdot 2^9\,\pi^6}\Big[v\Big(1080+5400/x+306/x^2-28/x^3+1/x^4\Big)+$$

$$+120\mathcal{L}_v\Big(18x+15-6(3+1/x)\log(x)-32/x\Big)-1440\mathcal{L}_+\Big(3+1/x\Big)\Big],$$

$$\rho^{\langle\bar{q}q\rangle}(t)=-\frac{m_s m_Q^4}{3\cdot 2^4\pi^4}\Big[v\Big(\langle\bar{q}q\rangle(24+2/x+1/x^2)-\langle\bar{s}s\rangle(6-7/x+1/x^2)\Big)+$$

$$-12\mathcal{L}_v\Big(\langle\bar{q}q\rangle(3-4x)+\langle\bar{s}s\rangle x\Big)\Big],$$

$$\rho^{\langle G^2\rangle}(t)=\frac{m_Q^4\langle G^2\rangle}{3\cdot 2^9\pi^6}\Big[v\Big(6+17/x+1/x^2\Big)+12\mathcal{L}_v\Big(x-\log(x)-1/x\Big)-24\mathcal{L}_+\Big],$$

$$\rho^{\langle\bar{q}Gq\rangle}(t)=\frac{m_s m_Q^2}{3\cdot 2^6\pi^4}\Big[v\Big(3\langle\bar{q}Gq\rangle-\langle\bar{s}Gs\rangle\Big)(8+1/x)+$$

$$+6\mathcal{L}_v\Big(\langle\bar{q}Gq\rangle(4x-1)-2\langle\bar{s}Gs\rangle x\Big)\Big],$$

$$\rho^{\langle\bar{q}q\rangle^2}(t)=\frac{m_Q^2\langle\bar{q}q\rangle^2}{6\pi^2}\,v\Big(2+1/x\Big),$$

$$\rho^{\langle G^3\rangle}(t)=\frac{m_Q^2\langle G^3\rangle}{5\cdot 3^2\cdot 2^9\pi^6}\Big[v\Big(310+415/x-6/x^2+2m_c^2\tau(1/x^3+8/x^2)\Big)+$$

$$+4\mathcal{L}_v\Big(155x-53-10(6+1/x)\log(x)-55/x-3m_c^2\tau/x^2\Big)-$$

$$-80\mathcal{L}_+\Big(6+1/x\Big)\Big].$$

Appendix B. Spectral function corresponding to the η_1 currents used in [81]

- $T_{QQ\bar{q}\bar{q}}$: $J^P=1^+$: $q\equiv u,d,s$

For this state, we use the tetraquark current given in Eq. (67).

$$\rho^{pert}=\frac{m_Q^8}{5\cdot 3^2\cdot 2^{10}\pi^6}\Big[v\Big(840x-7060-42302/x-8124/x^2-302/x^3+5/x^4\Big)+$$

$$+120\mathcal{L}_v\Big(14x^2-120x-177+18(7+4/x)\log(x)+256/x+33/x^2\Big)+$$

$$+4320\mathcal{L}_+\Big(7+4/x\Big)\Big],$$

$$\rho^{\langle\bar{q}q\rangle}(t)=\frac{m_q m_Q^4\langle\bar{q}q\rangle}{2^5\pi^4}\Big[v\Big(12x-46-50/x+3/x^2\Big)+24\mathcal{L}_v\Big(x^2-4x+5\Big)\Big],$$

$$\rho^{\langle G^2\rangle}(t)=\frac{m_Q^4\langle G^2\rangle}{3^3\cdot 2^{10}\pi^6}\Big[v\Big(78x-815-1192/x-69/x^2\Big)+$$

$$+6\mathcal{L}_v\Big(26x^2-276x+111+135\log(x)+128/x\Big)+1620\mathcal{L}_+\Big],$$

$$\rho^{\langle\bar{q}Gq\rangle}(t)=\frac{19m_q m_Q^2\langle\bar{q}Gq\rangle}{3^2\cdot 2^4\pi^4}\,v\Big(4-1/x\Big),$$

$$\rho^{\langle\bar{q}q\rangle^2}(t) = \frac{2m_Q^2\langle\bar{q}q\rangle^2}{9\pi^2}\, v\Big(4-1/x\Big)$$

$$\rho^{\langle G^3\rangle}(t) = -\frac{m_Q^2\langle G^3\rangle}{5\cdot 3^5\cdot 2^{10}\pi^6}\Bigg[v\Big(2820x-12850-15350/x-225/x^2+ +108m_Q^2\tau\,(1/x^3+26/x^2)\Big)+24\mathcal{L}_v\Big(235x^2-1110x+810+ +30(6+1/x)\log(x)+265/x-54m_c^2\tau\,(1/x^2+1/x)\Big)+ 1440\mathcal{L}_+\Big(6+1/x\Big)\Bigg].$$

- $T_{QQ\bar{u}\bar{s}}$: $J^P = 1^+$

$$\rho^{pert}(t) = \frac{m_Q^8}{5\cdot 3^2\cdot 2^{11}\,\pi^6}\Bigg[v\Big(840x-7060-42302/x-8124/x^2-302/x^3+5/x^4\Big)+ +120\mathcal{L}_v\Big(14x^2-120x-177+18(7+4/x)\log(x)+256/x+33/x^2\Big)+ +4320\mathcal{L}_+\Big(7+4/x\Big)\Bigg],$$

$$\rho^{\langle\bar{q}q\rangle}(t) = \frac{m_s m_Q^4}{3\cdot 2^7\pi^4}\Big(2\langle\bar{q}q\rangle+\langle\bar{s}s\rangle\Big)\Bigg[v\Big(12x-46-50/x+3/x^2\Big)+ +24\mathcal{L}_v\Big(x^2-4x+5\Big)\Bigg],$$

$$\rho^{\langle G^2\rangle}(t) = \frac{m_Q^4\langle G^2\rangle}{3^3\cdot 2^{11}\pi^6}\Bigg[v\Big(78x-815-1192/x-69/x^2\Big)+ +6\mathcal{L}_v\Big(26x^2-276x+111+135\log(x)+128/x\Big)+1620\mathcal{L}_+\Bigg],$$

$$\rho^{\langle\bar{q}Gq\rangle}(t) = \frac{m_s m_Q^2}{3^2\cdot 2^6\pi^4}\Big(12\langle\bar{q}Gq\rangle+7\langle\bar{s}Gs\rangle\Big)\, v\Big(4-1/x\Big),$$

$$\rho^{\langle\bar{q}q\rangle^2}(t) = \frac{m_Q^2\langle\bar{q}q\rangle\langle\bar{s}s\rangle}{9\pi^2}\, v\Big(4-1/x\Big),$$

$$\rho^{\langle G^3\rangle}(t) = -\frac{m_Q^2\langle G^3\rangle}{5\cdot 3^5\cdot 2^{11}\pi^6}\Bigg[v\Big(2820x-12850-15350/x-225/x^2+ +108m_Q^2\tau\,(1/x^3+26/x^2)\Big)+24\mathcal{L}_v\Big(235x^2-1110x+810+ +30(6+1/x)\log(x)+265/x-54m_c^2\tau\,(1/x^2+1/x)\Big)+ 1440\mathcal{L}_+\Big(6+1/x\Big)\Bigg].$$

- $T_{QQ\bar{q}\bar{q}}$ or $T_{QQ\bar{s}\bar{s}}$: $J^P = 0^+$

For this state, we use the tetraquark current given in Eq. (68). We obtain:

$$\rho^{pert}(t) = -\frac{m_Q^8}{5\cdot 3\cdot 2^9\pi^6}\Big[v\Big(720+6420/x+1434/x^2+58/x^3-1/x^4\Big)+$$
$$+120\mathcal{L}_v\Big(12x+33-6(3+2/x)\log(x)-40/x-6/x^2\Big)-$$
$$-1440\mathcal{L}_+\Big(3+2/x\Big)\Big],$$
$$\rho^{\langle\bar{q}q\rangle}(t) = -\frac{m_q m_Q^4\langle\bar{q}q\rangle}{8\pi^4}\Big[v\Big(12+16/x-1/x^2\Big)+12\mathcal{L}_v\Big(2x-3\Big)\Big],$$
$$\rho^{\langle G^2\rangle}(t) = -\frac{m_Q^4\langle G^2\rangle}{3\cdot 2^9\pi^6}\Big[v\Big(30+31/x+5/x^2\Big)+$$
$$+6\mathcal{L}_v\Big(10x-6-(5-1/x)\log(x)-4/x\Big)-12\mathcal{L}_+\Big(5-1/x\Big)\Big],$$
$$\rho^{\langle\bar{q}Gq\rangle}(t) = \frac{19m_q m_Q^2\langle\bar{q}Gq\rangle}{3\cdot 2^5\pi^4}v\Big(4-1/x\Big),$$
$$\rho^{\langle\bar{q}q\rangle^2}(t) = \frac{m_Q^2\langle\bar{q}q\rangle^2}{3\pi^2}\,v\Big(4-1/x\Big),$$
$$\rho^{\langle G^3\rangle}(t) = -\frac{m_Q^2\langle G^3\rangle}{5\cdot 3^3\cdot 2^8\pi^6}\Big[v\Big(430+495/x-6/x^2+3m_Q^2\tau\,(1/x^3+26/x^2)\Big)+$$
$$+\mathcal{L}_v\Big(860x-232-5(87+10/x)\log(x)-285/x-36m_c^2\tau\,(1/x^2+1/x)\Big)-$$
$$-10\mathcal{L}_+\Big(87+10/x\Big)\Big].$$

- $T_{QQ\bar{q}\bar{s}}$: $J^P = 0^+$

For this state, we use the tetraquark current given in Eq. (68). We obtain:

$$\rho^{pert}(t) = -\frac{m_Q^8}{5\cdot 3\cdot 2^{10}\pi^6}\Big[v\Big(720+6420/x+1434/x^2+58/x^3-1/x^4\Big)+$$
$$+120\mathcal{L}_v\Big(12x+33-6(3+2/x)\log(x)-40/x-6/x^2\Big)-$$
$$-1440\mathcal{L}_+\Big(3+2/x\Big)\Big],$$
$$\rho^{\langle\bar{q}q\rangle}(t) = -\frac{m_s m_Q^4}{3\cdot 2^5\pi^4}\Big(2\langle\bar{q}q\rangle+\langle\bar{s}s\rangle\Big)\Big[v\Big(12+16/x-1/x^2\Big)+12\mathcal{L}_v\Big(2x-3\Big)\Big],$$
$$\rho^{\langle G^2\rangle}(t) = -\frac{m_Q^4\langle G^2\rangle}{3\cdot 2^{10}\pi^6}\Big[v\Big(30+31/x+5/x^2\Big)+$$
$$+6\mathcal{L}_v\Big(10x-6-(5-1/x)\log(x)-4/x\Big)-12\mathcal{L}_+\Big(5-1/x\Big)\Big],$$

$$\rho^{\langle\bar{q}Gq\rangle}(t)=\frac{m_s m_Q^2}{3\cdot 2^7\pi^4}\Big(12\langle\bar{q}Gq\rangle+7\langle\bar{s}Gs\rangle\Big)\,v\Big(4-1/x\Big),$$

$$\rho^{\langle\bar{q}q\rangle^2}(t)=\frac{m_Q^2\langle\bar{q}q\rangle\langle\bar{s}s\rangle}{6\pi^2}\,v\Big(4-1/x\Big),$$

$$\rho^{\langle G^3\rangle}(t)=-\frac{m_Q^2\langle G^3\rangle}{5\cdot 3^3\cdot 2^9\pi^6}\Bigg[v\Big(430+495/x-6/x^2+3m_Q^2\tau\,(1/x^3+26/x^2)\Big)+$$
$$+\mathcal{L}_v\Big(860x-232-5(87+10/x)\log(x)-285/x-36m_c^2\tau\,(1/x^2+1/x)\Big)-$$
$$-10\mathcal{L}_+\Big(87+10/x\Big)\Bigg].$$

Appendix C. Spectral function of $T^{1^+}_{QQ\bar{q}\bar{s}}$ corresponding to the current in Eq. (70) used in [82]

$$\rho^{pert}(t)=\frac{m_Q^8}{3^4\cdot 2^{16}\pi^6}\Bigg[v\Big(2520x+420+19128/x-2016/x^2-454/x^3+13/x^4\Big)+$$
$$+24\mathcal{L}_v\Big(210x^2+363-6(51+8/x)\log(x)-592/x+99/x^2\Big)-$$
$$-288\mathcal{L}_+\Big(51+8/x\Big)\Bigg]+-\frac{m_s m_Q^7}{3^3\cdot 2^{12}\pi^6}\Bigg[v\Big(60+130/x-18/x^2-1/x^3\Big)+$$
$$+12\mathcal{L}_v\Big(10x-4-6\log(x)-6/x+1/x^2\Big)-144\mathcal{L}_+\Bigg],$$

$$\rho^{\langle\bar{q}q\rangle}(t)=\frac{7m_Q^5}{3^4\cdot 2^{10}\pi^4}\Bigg[\langle\bar{q}q\rangle\Big(v(60x+10-34/x-9/x^2)+24\mathcal{L}_v(5x^2-3+2/x)\Big)+$$
$$+12\langle\bar{s}s\rangle\Big(v(6-5/x-1/x^2)+6\mathcal{L}_v(2x-2+1/x)\Big)\Bigg]-$$
$$-\frac{m_s m_Q^4}{3^3\cdot 2^{12}\pi^4}\Bigg[8\langle\bar{q}q\rangle\Big(v(156+68/x+1/x^2)+12\mathcal{L}_v(26x-25)\Big)-$$
$$-\langle\bar{s}s\rangle\Big(v(204x+34-322/x+39/x^2)+24\mathcal{L}_v(17x^2+11)\Big)\Bigg],$$

$$\rho^{\langle G^2\rangle}(t)=\frac{m_Q^4\langle G^2\rangle}{3^5\cdot 2^{16}\pi^6}\Bigg[v\Big(2130x+355-712/x-234/x^2\Big)+$$
$$+6\mathcal{L}_v\Big(710x^2-369-27\log(x)+200/x\Big)-324\mathcal{L}_+\Bigg],$$

$$\rho^{\langle\bar{q}Gq\rangle}(t)=-\frac{m_Q^3}{3^4\cdot 2^{12}\pi^4}\Bigg[2\langle\bar{q}Gq\rangle\Big(v(174x+29-53/x)+6\mathcal{L}_v(58x^2+36-7/x)\Big)+$$
$$-\langle\bar{s}Gs\rangle\Big(v(48x+14+493/x)+12\mathcal{L}_v(8x^2+x-84)\Big)\Bigg]+$$
$$+\frac{m_s m_Q^2}{3^4\cdot 2^{12}\pi^4}\Bigg[\langle\bar{q}Gq\rangle\Big(9v(68+5/x)-6\mathcal{L}_v(84x-39)\Big)-$$

$$-\langle\bar{s}Gs\rangle\Big(8v(3x-10+7/x)+6\mathcal{L}_v(8x^2+4x+9)\Big)\Big],$$

$$\rho^{\langle\bar{q}q\rangle^2}(t)=\frac{m_Q^2\langle\bar{q}q\rangle\langle\bar{s}s\rangle}{3^3\cdot 2^6\pi^2}\,v\Big(24+1/x\Big)-\frac{7m_sm_Q\langle\bar{q}q\rangle\langle\bar{s}s\rangle}{3^3\cdot 2^6\pi^2}\,v\,s\,\tau\,,$$

$$\rho^{\langle G^3\rangle}(t)=-\frac{m_Q^2\langle G^3\rangle}{5\cdot 3^8\cdot 2^{16}\pi^6}\Big[v\Big(5(211680x^3-277200x^2+87288x-77680-$$
$$-89312/x-1215/x^2)-12m_Q^2\tau(14700x^2-10150x+2170-105/x+$$
$$+792/x^2-144/x^3)\Big)+12\mathcal{L}_v\Big(5\big(35280x^4-52080x^3+22052x^2-$$
$$-15138x+4593+6(729+116/x)\log(x)+4274/x\big)-$$
$$-24m_Q^2\tau(1225x^3-1050x^2+315x-35-54/x+9/x^2)\Big)+$$
$$+720(729+116/x)\mathcal{L}_+\Big].$$

Note that the spectral function related to the current:

$$\mathcal{O}^{8,\mu}_{T,2}=(\bar{Q}_j\gamma_5\frac{\lambda_a^{jk}}{2}u_k)(Q_m\,i\gamma^\mu\frac{\lambda_a^{mn}}{2}\bar{d}_n)$$

used in Eq. (3) of Ref. [82] can be deduced from the previous expression by changing s to d, q to u and by taking $m_s\equiv m_d=0$.

References

[1] M. Gell-Mann, Phys. Lett. 8 (1964) 214.
[2] G. Zweig, CERN-TH-401 and TH-412 (1964), in: D.B. Lichtenberg, S.P. Rosen (Eds.), Developments in Quark Theory of Hadrons, vol. 1, Hadronic Press, MA, 1980.
[3] G.C. Rossi, G. Veneziano, Nucl. Phys. B 123 (1977) 507;
G.C. Rossi, G. Veneziano, QCD20-Montpellier, arXiv:2011.09774, 27–30 October 2020.
[4] R.L. Jaffe, Phys. Rev. D 15 (1977) 267; Phys. Rep. 409 (2005) 1 and references therein.
[5] J.D. Weinstein, N. Isgur, Phys. Rev. D 27 (1983) 588.
[6] N.N. Achasov, S.A. Devyanin, G.N. Shestakov, Sov. J. Nucl. Phys. 32 (1980) 566.
[7] G.f Hooft, G. Isidori, L. Maiani, A.D. Polosa, V. Riquer, Phys. Lett. B 662 (2008) 424.
[8] S. Weinberg, Phys. Rev. Lett. 110 (2013) 261601.
[9] M. Knecht, S. Peris, Phys. Rev. D 88 (2013) 036016.
[10] J.I. Latorre, P. Pascual, J. Phys. G 11 (1985) 231.
[11] S. Narison, Phys. Lett. B 175 (1986) 88.
[12] S. Narison, Nucl. Phys. A 1017 (2022) 122337.
[13] S. Narison, G. Veneziano, Int. J. Mod. Phys. A 4 (11) (1989) 2751;
A. Bramon, S. Narison, Mod. Phys. Lett. A 4 (1989) 1113.
[14] S. Narison, Nucl. Phys. B 509 (1998) 312;
S. Narison, Nucl. Phys. B, Proc. Suppl. 64 (1998) 210.
[15] P. Minkowski, W. Ochs, Eur. Phys. J. C 9 (1999) 283.
[16] G. Mennessier, S. Narison, W. Ochs, Phys. Lett. B 665 (2008) 205;
G. Mennessier, S. Narison, X.-G. Wang, Phys. Lett. B 696 (2011) 40.
[17] R.M. Albuquerque, F. Fanomezana, S. Narison, A. Rabemananjara, Phys. Lett. B 715 (2012) 129.
[18] R.M. Albuquerque, S. Narison, F. Fanomezana, A. Rabemananjara, D. Rabetiarivony, G. Randriamanatrika, Int. J. Mod. Phys. A 31 (2016) 1650196.
[19] R.M. Albuquerque, F. Fanomezana, S. Narison, A. Rabemananjara, Int. J. Mod. Phys. A 31 (17) (2016) 1650093; Nucl. Part. Phys. Proc. 300–302 (2018) 186.

[20] R.M. Albuquerque, S. Narison, D. Rabetiarivony, G. Randriamanatrika, Int. J. Mod. Phys. A 33 (16) (2018) 1850082;
R.M. Albuquerque, S. Narison, D. Rabetiarivony, G. Randriamanatrika, Nucl. Part. Phys. Proc. 282–284 (2017) 83.
[21] R.M. Albuquerque, S. Narison, A. Rabemananjara, D. Rabetiarivony, G. Randriamanatrika, Phys. Rev. D 102 (2020) 094001;
R.M. Albuquerque, S. Narison, A. Rabemananjara, D. Rabetiarivony, G. Randriamanatrika, arXiv:2102.08776 [hep-ph], 2021.
[22] R. Albuquerque, S. Narison, D. Rabetiarivony, G. Randriamanatrika, Nucl. Phys. A 1007 (2021) 122113;
R. Albuquerque, S. Narison, D. Rabetiarivony, G. Randriamanatrika, arXiv:2102.04622 [hep-ph], 2021;
R. Albuquerque, S. Narison, D. Rabetiarivony, G. Randriamanatrika, Nucl. Part. Phys. Proc. 312 (317) (2021) 125;
S. Narison, D. Rabetiarivony, A. Rabemananjara, arXiv:2111.06481 [hep-ph], 2021.
[23] R. Albuquerque, S. Narison, D. Rabetiarivony, Phys. Rev. D 103 (7) (2021) 074015.
[24] S. Narison, D. Rabetiarivony, arXiv:2110.05956 [hep-ph], 2021.
[25] M.A. Shifman, A.I. Vainshtein, V.I. Zakharov, Nucl. Phys. B 147 (1979) 385; Nucl. Phys. B 147 (1979) 448.
[26] V.I. Zakharov, Sakurai's price, Int. J. Mod. Phys. A 14 (1999) 4865.
[27] S. Narison, QCD Spectral Sum Rules, World Sci. Lect. Notes Phys., vol. 26, ISBN 9780521037310, 1989, p. 1.
[28] S. Narison, QCD as a Theory of Hadrons, Cambridge Monogr. Part. Phys. Nucl. Phys. Cosmol., vol. 17, 2004, pp. 1–778, arXiv:hep-ph/0205006.
[29] S. Narison, Phys. Rep. 84 (1982) 263; Acta Phys. Pol. B 26 (1995) 687; Riv. Nuovo Cimento 10 (2) (1987) 1; Nucl. Part. Phys. Proc. 258–259 (2015) 189; Nucl. Part. Phys. Proc. 207 (208) (2010) 315.
[30] B.L. Ioffe, Prog. Part. Nucl. Phys. 56 (2006) 232.
[31] L.J. Reinders, H. Rubinstein, S. Yazaki, Phys. Rep. 127 (1985) 1.
[32] E. de Rafael, les Houches summer school, arXiv:hep-ph/9802448, 1998.
[33] R.A. Bertlmann, Acta Phys. Austriaca 53 (1981) 305.
[34] F.J. Yndurain, The Theory of Quark and Gluon Interactions, 3rd edition, Springer, New York, 1999.
[35] P. Pascual, R. Tarrach, QCD: Renormalization for Practitioner, Springer, New York, 1984.
[36] H.G. Dosch, in: S. Narison (Ed.), Non-perturbative Methods, World Scientific, Singapore, 1985.
[37] P. Colangelo, A. Khodjamirian, in: M. Shifman (Ed.), At the Frontier of Particle Physics: Handbook of QCD, vol. 1495, World Scientific, Singapore, 2001.
[38] J.S. Bell, R.A. Bertlmann, Nucl. Phys. B 177 (1981) 218; Nucl. Phys. B 187 (1981) 285.
[39] S. Narison, E. de Rafael, Phys. Lett. B 522 (2001) 266.
[40] LHCb collaboration, R. Aaij, et al., Sci. Bull. 65 (2020) 1983.
[41] LHCb collaboration, R. Aaij, et al., Phys. Rev. Lett. 125 (2020) 242001; Phys. Rev. D 102 (2020) 112003.
[42] BES III collaboration, M. Ablikim, et al., Phys. Rev. Lett. 126 (2021) 102001.
[43] LHCb collaboration, R. Aaij, et al., arXiv:2109.01056.
[44] S. Narison, Nucl. Phys. A 1020 (2022) 122393.
[45] S. Narison, Phys. Lett. B 210 (1988) 238.
[46] S. Narison, Phys. Lett. B 322 (1994) 247.
[47] S. Narison, Phys. Lett. B 387 (1996) 162.
[48] R.M. Albuquerque, S. Narison, M. Nielsen, Phys. Lett. B 684 (2010) 236;
R.M. Albuquerque, S. Narison, Phys. Lett. B 694 (2011) 274.
[49] R.D. Matheus, S. Narison, M. Nielsen, J.-M. Richard, Phys. Rev. D 75 (2007) 014005.
[50] J.M. Dias, S. Narison, F.S. Navarra, M. Nielsen, J.-M. Richard, Phys. Lett. B 703 (2011) 274.
[51] S. Narison, F.S. Navarra, M. Nielsen, Phys. Rev. D 83 (2011) 016004.
[52] S. Narison, Int. J. Mod. Phys. A 33 (10) (2018) 1850045; Addendum: Int. J. Mod. Phys. A 33 (2018) 1850045 and references therein.
[53] S. Narison, arXiv:1812.09360, 2018.
[54] S. Narison, Nucl. Part. Phys. Proc. 312 (317) (2021) 87;
S. Narison, Nucl. Part. Phys. Proc. 300–302 (2018) 153.
[55] S. Narison, Phys. Lett. B 802 (2020) 135221.
[56] S. Narison, Phys. Lett. B 784 (2018) 261.
[57] S. Narison, Phys. Lett. B 721 (2013) 269;
S. Narison, Phys. Lett. B 718 (2013) 1321;
S. Narison, Nucl. Part. Phys. Proc. 234 (2013) 187.
[58] S. Narison, Phys. Lett. B 693 (2010) 559;
Erratum: S. Narison, Phys. Lett. B 705 (2011) 544.

[59] S. Narison, Phys. Lett. B 706 (2012) 412;
S. Narison, Phys. Lett. B 707 (2012) 259.
[60] S. Narison, Int. J. Mod. Phys. A 30 (2015) 1550116; Phys. Lett. B 738 (2014) 346.
[61] R.M. Albuquerque, S. Narison, Phys. Lett. B 694 (2010) 217;
R.M. Albuquerque, S. Narison, M. Nielsen, Phys. Lett. B 684 (2010) 236.
[62] B.L. Ioffe, Nucl. Phys. B 188 (1981) 317; Erratum: Nucl. Phys. B 191 (1981) 591.
[63] Y. Chung, et al., Z. Phys. C 25 (1984) 151.
[64] H.G. Dosch, M. Jamin, S. Narison, Phys. Lett. B 220 (1989) 251.
[65] A.A. Ovchinnikov, A.A. Pivovarov, Yad. Fiz. 48 (1988) 1135.
[66] S. Narison, Phys. Lett. B 605 (2005) 319.
[67] G. Launer, S. Narison, R. Tarrach, Z. Phys. C 26 (1984) 433.
[68] S. Narison, R. Tarrach, Phys. Lett. B 125 (1983) 217.
[69] R.A. Bertlmann, G. Launer, E. de Rafael, Nucl. Phys. B 250 (1985) 61.
[70] S. Narison, Phys. Lett. B 673 (2009) 30.
[71] P.A. Zyla, et al., Particle Data Group, Prog. Theor. Exp. Phys. 2020 (2020) 083C01.
[72] R.D. Matheus, F.S. Navarra, M. Nielsen, C.M. Zanetti, Phys. Rev. D 80 (2009) 056002.
[73] R.M. Albuquerque, J.M. Dias, K.P. Khemchandanic, A.M. Torres, F.S. Navarra, M. Nielsen, C.M. Zanetti, J. Phys. G 46 (9) (2019) 093002.
[74] H.X. Chen, W. Chen, X. Liu, S.-L. Zhu, Phys. Rep. 639 (2016) 1;
Y.-R. Liu, H.-X. Chen, W. Chen, X. Liu, S.-L. Zhu, Prog. Part. Nucl. Phys. 107 (2019) 237.
[75] R.M. Albuquerque, PhD Thesis, Univ. Montpellier, 2013, arXiv:1306.4671 [hep-ph].
[76] W. Chen, H.-y. Jin, R.T. Kleiv, T.G. Steele, M. Wang, Q. Xu, Phys. Rev. D 88 (2013) 045027;
W. Chen, T.G. Steele, H.-X. Chen, S.-L. Zhu, Phys. Rev. D 92 (2015) 054002.
[77] F.S. Navarra, M. Nielsen, S.H. Lee, Phys. Lett. B 649 (2007) 166.
[78] Z.-G. Wang, Z.H. Yan, Eur. Phys. J. C 78 (2018) 19;
Z.-G. Wang, Acta Phys. Pol. 49 (2018) 1781.
[79] Z.-G. Wang, Y.-M. Xu, H.-J. Wang, Commun. Theor. Phys. 55 (2011) 1049.
[80] S.S. Agaev, K. Azizi, H. Sundu, arXiv:2108.00188, 2021;
S.S. Agaev, K. Azizi, H. Sundu, Turk. J. Phys. 44 (2) (2020) 95.
[81] M.-L. Du, W. Chen, X.-L. Chen, S.L. Zhu, Phys. Rev. D 87 (2013) 014003.
[82] L. Tang, B.-D. Wan, K. Maltman, C.-F. Qiao, Phys. Rev. D 101 (2020) 094032.
[83] BELLE collaboration, A. Garmash, et al., Phys. Rev. D 91 (2015) 072003;
A. Bondar, et al., Phys. Rev. Lett. 108 (2012) 122001.
[84] A. Ali, L. Maiani, A.D. Polosa, Multiquark Hadrons, Cambridge Univ. Press, ISBN 9781316761465, 2019.
[85] J.-M. Richard, Few-Body Syst. 57 (12) (2016) 1185;
J.-M. Richard, Nucl. Part. Phys. Proc. 312 (317) (2021) 146.
[86] E.S. Swanson, Phys. Rep. 429 (2006) 243.
[87] F.K. Guo, C. Hanhart, U.-G. Meißner, Q. Wang, Q. Zhao, B.-S. Zou, Rev. Mod. Phys. 90 (2018) 015004.
[88] N. Brambilla, S. Eidelman, C. Hanhart, A. Nefediev, C.-P. Shen, C.E. Thomas, A. Vairo, C.-Z. Yuan, Phys. Rep. 873 (2020) 1.
[89] P. Junnarkar, N. Mathur, M. Padmanath, Phys. Rev. D 99 (3) (2019) 034507.
[90] A. Francis, R.J. Hudspith, R. Lewis, K. Maltman, Phys. Rev. Lett. 118 (14) (2017) 142001.
[91] P. Mohanta, S. Basak, Phys. Rev. D 102 (2020) 094516.
[92] L. Leskovec, S. Meinel, M. Pflaumer, M. Wagner, Phys. Rev. D 100 (2019) 014503.
[93] H.G. Dosch, S.J. Brodsky, G.F. de Téramond, M. Nielsen, L. Zou, Nucl. Part. Phys. Proc. 312 (317) (2021) 135.
[94] Q. Meng, E. Hiyama, A. Hosaka, M. Oka, P. Gubler, K.U. Can, T.T. Takahashi, H.S. Zong, Phys. Lett. B 814 (2021) 136095.
[95] M. Karliner, J.L. Rosner, Phys. Rev. D 90 (9) (2014) 094007.
[96] E.J. Eichten, C. Quigg, Phys. Rev. Lett. 119 (20) (2017) 202002.
[97] D. Ebert, R.N. Faustov, V.O. Galkin, W. Lucha, Phys. Rev. D 76 (2007) 114015.
[98] E. Braaten, L.-P. He, A. Mohapatra, Phys. Rev. Lett. D 103 (2021) 016001.
[99] J.-B. Cheng, S.-Y. Li, Y.-R. Liu, Z.G. Si, T. Yao, Chin. Phys. C 45 (2021) 043102.
[100] E. Hernandez, J. Vijande, A. Valcarce, J.-M. Richard, Phys. Lett. B 800 (2020) 135073.
[101] X.-Z. Weng, W.-Z. Deng, S.-L. Zhu, arXiv:2108.07242 [hep-ph].
[102] Y. Wu, X. Jin, R. Liu, H. Huang, J. Ping, arXiv:2112.05967, 2021.
[103] P. Bicudo, K. Cichy, A. Peters, M. Wagner, Phys. Rev. D 93 (2016) 034501.